

# Advances and Outlooks of Heat Transfer Enhancement by Longitudinal Vortex Generators <sup>a</sup>

Ya-Ling He <sup>a</sup> and Yuwen Zhang <sup>a, b</sup>

<sup>a</sup> Key Laboratory of Thermal-Fluid Science and Engineering of MOE, School of Energy and Power Engineering, Xi'an Jiaotong University, Xi'an, Shaanxi, 710049, P.R. China

<sup>b</sup> Department of Mechanical and Aerospace Engineering, University of Missouri, Columbia, MO 65211, USA

## Abstract

In the last several decades, heat transfer enhancements using extended surface (fins) has received considerable attentions. A new heat transfer enhancement technique, longitudinal vortex generators (LVG), has received significant attention since the 1990s. It is activated by a special type of extended surface that can generate vortices with axes parallel to the main flow direction. The vortices result from strong swirling secondary flow caused by flow separation and friction. The state-of-the-art on research and applications of LVG are described here. The topical coverage includes heat transfer enhancement in straight channels and in heat exchangers. Among the latter are plate and wavy fin-and-tube heat exchangers, fin-and-oval-tube heat exchangers, and fin-and-tube heat exchangers with multiple rows of tubes. The trends and future directions of heat transfer enhancement by means of LVG are discussed.

**Keywords:** heat transfer, channels, enhancement, longitudinal vortex generators, shell-and-tube heat exchangers.

## Nomenclature

$A$	area ( $\text{m}^2$ )
$c_p$	specific heat ( $\text{J}/\text{kg}\cdot\text{K}$ )
$D$	tube outer diameter (m)
$D_h$	hydraulic diameter (m)
$f$	friction coefficient
$H$	channel height (m)
$h$	heat transfer coefficient ( $\text{W}/\text{m}^2\cdot\text{K}$ )
$j$	Colburn $j$ factor
$L$	channel length (m)
$I$	row number
$\text{Nu}$	Nusselt number
$p$	pressure (Pa)
$Q$	heat transfer rate (W)
$\text{Re}$	Reynolds number
$T$	temperature (K)
$u$	velocities in the x-direction
$v$	velocities in the y-direction
$w$	velocities in the z-direction
$x, y, z$	coordinate (m)

## Greek Symbols

$\alpha$	angel of attack (°)
$\Delta p$	air side pressure drop (Pa)
$\Lambda$	aspect ratio
$\nu$	viscosity ( $\text{m}^2/\text{s}$ )
$\theta$	wavy angle or average interaction angle (°)
$\rho$	density ( $\text{kg}/\text{m}^3$ )

### *Subscripts*

0	baseline case
m	mean value
x	local value

### *Abbreviations*

CFD	common flow down
CFU	common flow up
LVG	longitudinal vortex generator
RWP	rectangular winglet pairs

## 1. Introduction

Gas-gas and gas-liquid heat exchangers find wide applications in fields such as HVAC, refrigeration, electronics cooling, food processing, automotives, petroleum, aerospace, and spaceflight. The overall performance of heat exchangers is often limited by low heat transfer coefficients on the gas side, which results in a corresponding low efficiency of energy utilization. The more exacting needs of modern industry and the necessity for more effective global energy utilization call for more compact heat exchangers to achieve lower energy consumption. Thus, it is very imperative to develop heat transfer enhancement techniques with low pressure drops.

Increase of the heat transfer coefficient on the gas side can be achieved by various techniques, either passive or active [1]. Passive techniques, such as fins, treated or rough surfaces, swirl-flow devices, and additives to the fluid, do not require any external power for their implementation. These techniques are, however, sources of additional pressure drop. Active techniques, such as vibration, electromagnetic fields, and jet impingement, do require additional power for their implementation and may also give rise to pressure drop increases.

In the last several decades, heat transfer enhancement using extended surface (fins) has received considerable attentions. The traditional fins include wavy, perforated, slit, louvered, and composite fins, which alter the geometric configuration to improve the flow and heat transfer performances.

A new heat transfer enhancement technique, longitudinal vortex generator (LVG), has received more and more attention since the 1990s. It is a special type of extended surface that can generate vortices with their axes parallel to the main flow direction. The vortices are generated as a result of strong swirling secondary flow caused by flow separation and friction, such that there is a reduction in boundary layer thickness, swirling and flow destabilization, and increases of the temperature gradient near the heat transfer surface. It will be shown during the course of the review presented here that the heat transfer enhancement due to LVG can be achieved with moderate increases of pressure drop.

Due to the significant advantage of the use of LVGs, researchers across the globe have carried out systematic experimental and numerical studies on LVG and its applications in plate, channel, and fin-and-tube heat exchanges [2-17].

The state-of-the-art of LVG research with respect to heat transfer enhancement will be reviewed first, followed by a detailed summary of the research performed in the authors' laboratories. Finally, the trends and future directions on heat transfer enhancement LVG will be discussed.

## 2 Characteristics of Heat Transfer Enhancement by LVGs

To fulfill the requirements for environmentally friendliness, ease of use, compact, and energy saving, the heat exchangers must have low noise output, low power consumption, be compact, and highly stable. The heat exchanger must possess high heat capacity so that under the given load, heat transfer can be accomplished under small temperature differences and low flow velocity.

Under various constraints, the design goals can be met when the flow in the heat exchanger is laminar. From the perspective of the second law of thermodynamics, the entropy generation due to flow and heat transfer directly relates to the performance of the heat exchangers. Both a large temperature difference and a large pressure drop can result in significant entropy generation, which is undesirable. Therefore, the requirements of high heat transfer coefficient and low pressure drop coincide with the requirement of low entropy generation rate.

From microscopic point of view, the rate of entropy generation in the flow and heat transfer processes is related to the degree of disorder in the flow. Compared to the chaos of turbulent flow, laminar flow is more ordered and, therefore, using laminar flow in the heat exchanger decreases the rate of entropy production and thus improves the energy efficiency of the exchanger. Traditional techniques which are used to improve heat transfer efficiency include wavy, slit, or louvered fins, flow disruption, decreased boundary layer thickness, and interrupting the development of the boundary layer. These techniques can create small transverse vortices whose axes are perpendicular to the main flow direction. As Fiebig <sup>[16]</sup> pointed out, the heat transfer enhancement by transverse vortices is limited to the case of steady-state laminar flow. On the contrary, longitudinal vortices can significantly increase local and average heat transfer coefficients in the entire channel. Thus, LVGs have significant advantages for heat transfer enhancement in laminar flow in heat exchangers.

Figure 1 shows several common LVGs that include a delta wing, a rectangular wing, a delta winglet, and a rectangular winglet. As fluid passes across the LVG, strong secondary swirling flow is generated, and the tangential velocity of the vortices can be as high as two times the main flow velocity. The high-velocity swirling secondary flow not only promotes mixing of the fluids in the main flow and in the edge regions, but can also channel the high-energy fluid into the boundary layer to suppress and/or delay boundary layer separation, with a corresponding decrease of profile drag. By appropriate arrangement of LVGs, heat transfer on the air side of the heat exchanger can be enhanced while the pressure drop is decreased in some cases <sup>[8-9]</sup>. This counterintuitive outcome can be explained by the different effects of LVGs on the profile drag on the fins and the tubes. Although introduction of LVGs on the air side causes an increase of profile drag for the fins, properly designed LVGs can delay flow separation on the tube so that the profile drag for the tube is decreased. The results reported in [8-9] showed that the decrease of the drag on the tubes is greater than the increase of drag on the fins.

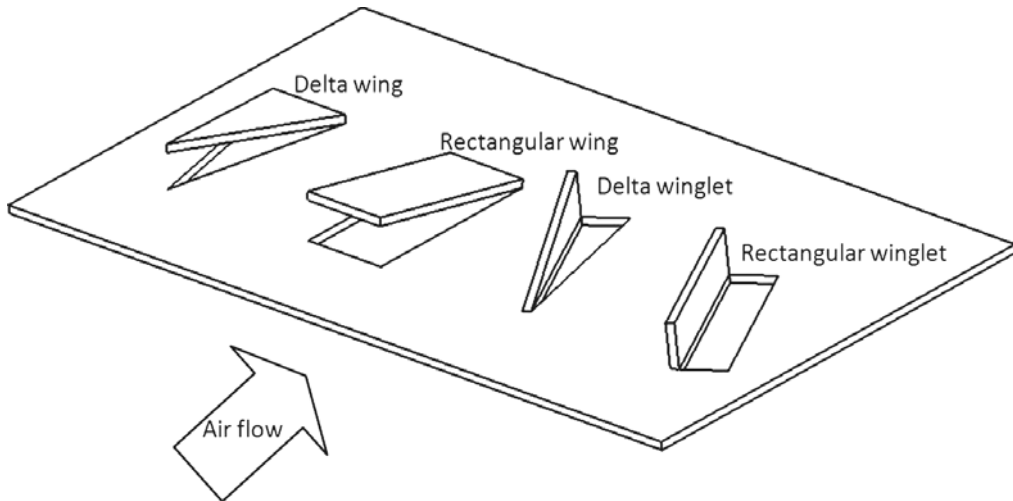


Fig. 1 Schematic diagrams of four common LVGs

### 3 Applications of LVGs for Heat Transfer Enhancement

The early studies of LVGs focused on their application to straight channels where the flow structures are relatively simple. While most early studies were performed experimentally, subsequent research made use of numerical simulation for the application of LVGs to fin-and-tube heat exchangers. These numerical investigations were made possible by the rapid development of computer hardware and software. The characteristics of fluid flow and heat transfer can now be thoroughly revealed by numerical simulation. Since there are only two or three rows of tubes in fin-and-tube heat exchangers for residential air conditioning systems, the numbers of rows in the early studies with LVGs were restricted to such numbers. More recently, the advent of other applications has led to the consideration of greater numbers of rows. The following discussion will encompass the applications LVGs to heat transfer enhancement in straight channels, plate and wavy fin-and-tube heat exchangers, fin-and-oval-tube heat exchangers, and fin-and-tube heat exchangers with multiple rows of tubes.

#### 3.1 Heat Transfer Enhancement in Flat-Plate Channels by LVGs

Dupont et al. <sup>[18]</sup> experimentally studied isothermal flow in a single channel of a compact heat exchanger equipped with embossed-type vortex generators in the transitional regime. Reynolds number defined using channel width as characteristic length ranged from 1000 to 5000. They suggested that smooth-shaped vortex generators are very promising for enhanced heat transfer. Heat transfer experiments were carried out by Gentry and Jacobi<sup>[19]</sup> in a channel equipped with delta wings and found that the local heat transfer coefficient in the secondary-flow region was increased by 300%, the average heat transfer coefficient for the channel as a whole was increased by 55%; the pressure drop was increased by 100% relative to the same channel without the delta-wing vortex generator. Liou and Chen<sup>[20]</sup> investigated heat transfer and fluid flow in a square duct with 12 different-shaped vortex generators using liquid crystal thermography and recommended LVGs with optimized geometric configurations. The Reynolds number that was defined based on channel hydraulic diameter and bulk mean velocity, was fixed at  $1.23 \times 10^4$ . Heat transfer enhancement in narrow rectangular channels was experimentally studied by Wang et al. <sup>[21]</sup> experimentally studied heat transfer enhancement in narrow rectangular channels with

longitudinal vortex generators and with water as working fluid. The overall heat transfer capability was increased by 10 – 45% due to LVGs. Fiebig<sup>[16]</sup> performed flow and heat transfer experiments in a rectangular channel with four types of LVGs and found that the longitudinal vortices resulted in a decrease in the critical Reynolds number by one or more orders of magnitude. The increased pressure loss were due to drag of the vortex generators, changes of the wall shear, and change in the momentum flux for the case of nonperiodic situations. Compared to delta or rectangular wings, delta and rectangular winglets resulted in even lower pressure drops for the same heat transfer rate. Zhu et al. <sup>[22]</sup> numerically investigated turbulent flows and heat transfer in a rib-roughened channel with longitudinal vortex generators using  $k-\epsilon$  model. The results showed that the combined effect of rib-roughness and vortex generators can enhance the average Nusselt number by nearly 450%; the increase of pressure drop can be as high as 44 times Hiravennavar et al. <sup>[23]</sup> also used numerical simulation to solve for the flow and heat transfer enhancement in a channel with a built-in rectangular winglet pair and found that the average Nusselt number for the entire channel was increased by 66.6% due to the rectangular winglet pair; the pressure drop was, however, not reported. Biswas et al. <sup>[17]</sup> determined the flow structure and heat transfer effects of longitudinal vortices in a channel flow both numerically and experimentally. The flow structure downstream of the LVGs was analyzed, and the angle of attack for optimized heat transfer performance ( $j/f$ ) was obtained.

Based on the existing research reported in the literatures, we systematically studied heat transfer enhancement by rectangular and delta winglet LVGs under common flow down (CFD) and common flow up (CFU) arrangements <sup>[24-25]</sup>. The mechanisms of heat transfer enhancement by LVGs were analyzed using the field synergy principle. The physical models for rectangular and delta winglets under two different arrangements were established (see Fig. 2) and the flow and heat transfer was numerically studied for isothermal wall with LVG deployment. A pair of LVGs are placed in the channel by either CFD or CFU arrangements. The working fluid was air with Prandtl number of 0.7. The shaded area in Fig. 2 was chosen as the computational domain due to symmetric condition.

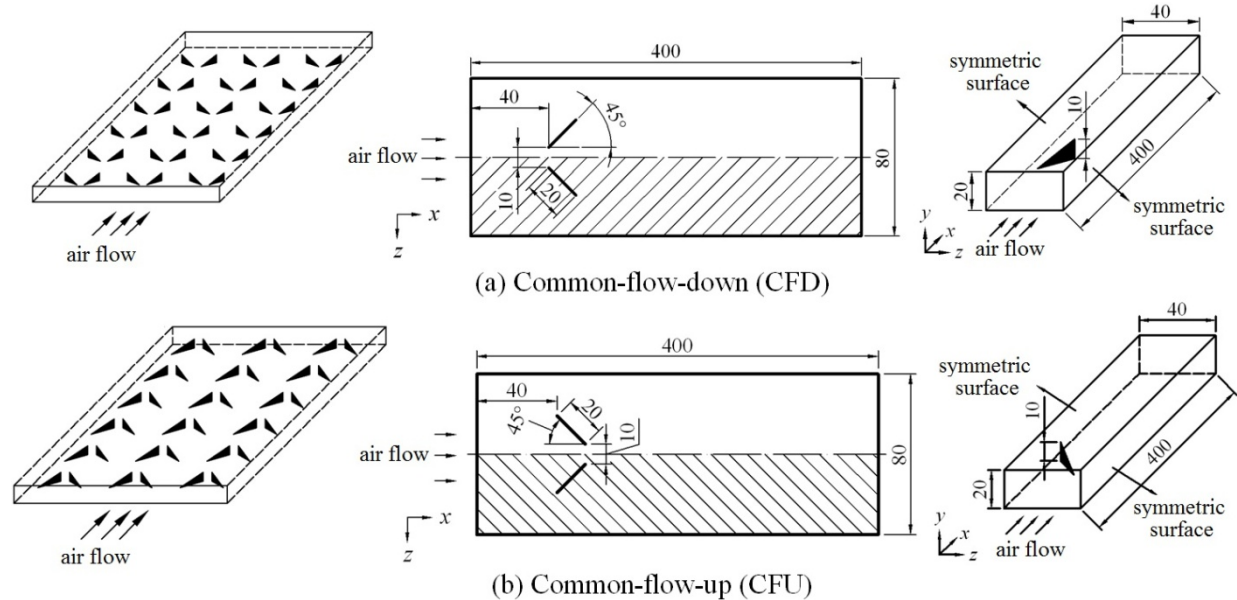


Fig. 2 Fluid flow and heat transfer in a channel with rectangular or delta winglets LVGs [24]

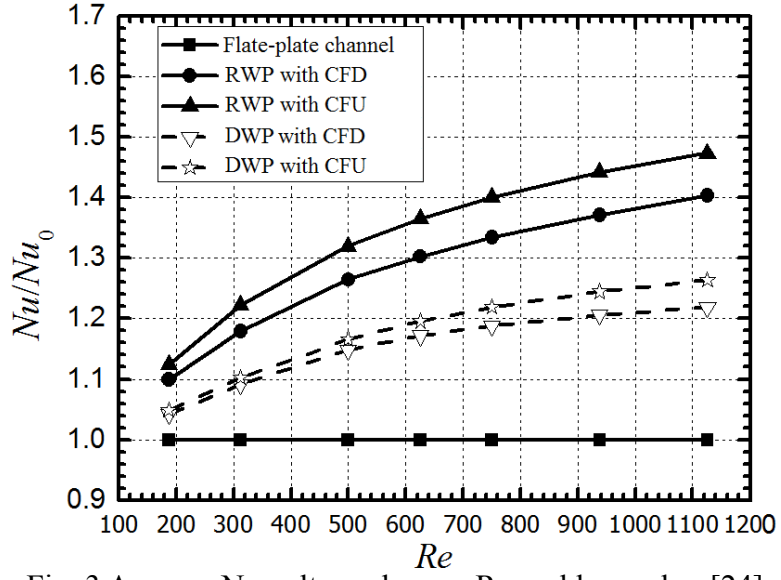


Fig. 3 Average Nusselt number vs. Reynolds number [24]

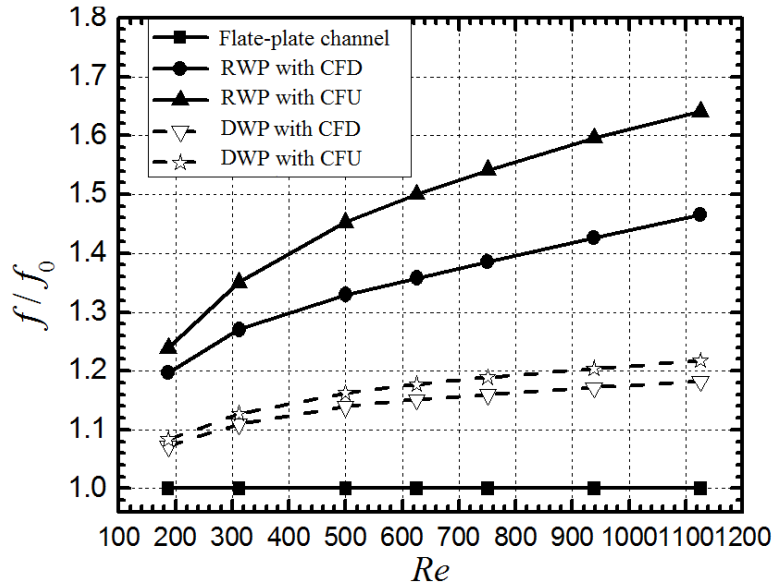


Fig. 4 Friction factor vs. Reynolds number [24]

Figure 3 shows the comparison of the ratio between average Nusselt number (with channel height as characteristic length) in a channel with LVGs (Nu) and smooth channel (Nu<sub>0</sub>). The Reynolds number is defined using mean velocity at the channel inlet and channel height. It can be seen that the Nusselt number is increased by 4 – 16% after adding LVGs in the channel. Under the same aspect ratio, the heat transfer enhancement by rectangular winglets is more significant than that of the delta winglets. The Nusselt number for CFU arrangement is higher than that for CFD arrangement. Thus, the effect of arrangement on Nusselt number for rectangular winglet is more significant than that for the delta winglet.

Variations of the ratio of f friction factor versus Reynolds number for different structures are

shown in Fig. 4. The friction factor is defined as  $f = [\Delta p / (\rho u_m^2 / 2)]H / L$ , where  $\Delta p$  is pressure drop,  $u_m$  is mean velocity at channel inlet,  $H$  is channel height and  $L$  is channel length. It can be seen that the friction factors for the channel with LVGs are higher than those of the smooth channel. The friction factors for the channel with rectangular winglets are much larger than for the case of delta winglets. For both rectangular and delta winglets, the friction factor for CFD arrangement is larger than that for the CFU arrangement. For delta winglets, the effect of arrangement on friction factor is not significant. On the contrary, the friction factors of the channel with rectangular winglets are more sensitive to how the winglets are arranged.

### 3.2 Heat Transfer Enhancement by LVGs in Fin-and-Tube Heat Exchangers

#### 3.2.1 Fin-and-Tube Heat Exchanger with Two Rows of Staggered Tube Banks

Sommers and Jacobi<sup>[26]</sup> added delta winglet LVGs to the evaporator of the refrigerator and experimentally studied the heat transfer performance. The results showed that the thermal resistance on the air side is decreased by 35 to 42% when the Reynolds number is between 500 and 1300. Leu et al. <sup>[27]</sup> experimentally and numerically studied heat transfer and fluid flow in fin-and-tube heat exchangers with a pair of block shaped vortex generators. The results showed that the optimized heat transfer performance is achieved when the attack angle of the longitudinal vortices is 45°: the Colburn  $j$  factor is increased by 8 – 30% while the friction factor,  $f$ , is only increased by 11 – 25%, which results in a reduction of the required heat transfer area by 25%. Allison and Dally <sup>[28]</sup> performed experimental studies the effect of a delta-winglet vortex generator pair on the performance of a tube-fin heat exchangers. Compared with the louvered fin-and-tube heat exchanger with the same size, the heat transfer capacity of the tube-and-fin heat exchanger is 87% of that of the louvered fin-and-tube heat exchanger, while the pressure drop the the former is only 53% of the latter. Zhang et al. <sup>[29]</sup> compared heat transfer performance of tube bank fin with mounted vortex generators to tube bank fin with punched vortex generators using the naphthalene sublimation technique. The results showed that the effects of different LVGs on the heat transfer performance are very limited.

Wu and Tao <sup>[30]</sup> numerically investigated laminar convection heat transfer in fin-and-tube heat exchangers in aligned arrangement with LVGs. They also optimized the angle of attack of the LVG and concluded that the overall heat transfer performance is maximized when the angle of attack is 30°.

The application of LVGs on fin-and-tube heat exchanger with two rows of tubes is not thoroughly investigated although it is widely used in the modern residential air conditional system. Therefore, we studied hydrodynamics and heat transfer characteristics of a novel heat exchanger with two rows of tubes and delta-winglet vortex generators <sup>[31]</sup>. Figure 5 shows the schematic diagram of the computational domain of the fin-and-tube heat exchanger with two rows of tubes, while the sizes of the computational domain are shown in Fig. 6. The mechanisms of flow and heat transfer in the heat exchanger will be analyzed first, and the effects of tube arrangements, angle of attack of the LVG, and the aspect ratio of the delta winglet on the heat transfer performance will be studied.

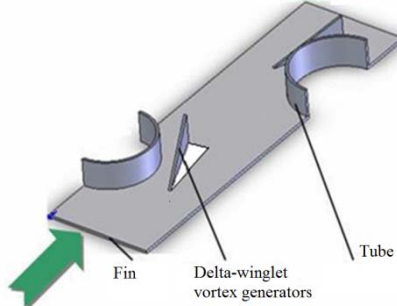


Fig. 5 Overview of the fin-and-tube heat exchanger and computational domain [31]

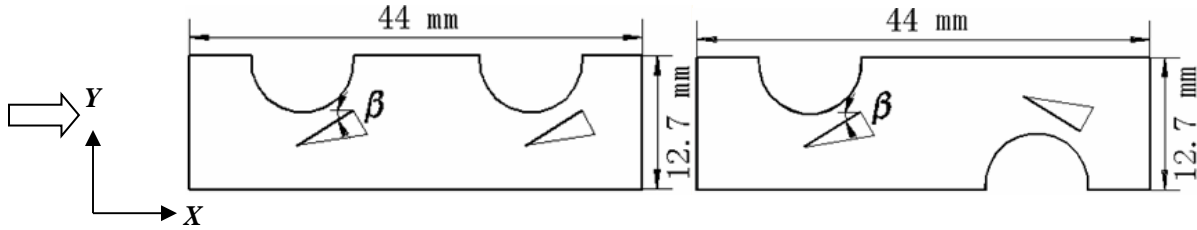


Fig. 6 Sizes of the computational domain [31]

### (1) Effects of Side Delta Winglets on Flow and Heat Transfer

The local flow field and temperature distribution in a fin-and-tube heat exchanger with side delta winglets will be analyzed first. It can be seen from Fig. 7 that a vortex whose axis is the same as the main flow direction is generated. When fluid flows across the delta winglet, the pressure difference across the delta winglet results in secondary flow and generates the vortex. The vortex disturbs the fluid flow and reduces the boundary layer thickness. Figure 8 shows velocity vector plots on a plane for both the enhanced and unenhanced configurations at  $Re = 1000$ . The plane is close to the bottom fin surface at a distance of  $z = 0.3$  mm from the bottom fin. It can be seen from Fig. 8 that the recirculation occurs widely behind the tubes, which further deteriorates the heat transfer. When the vortex generator with common-flow-up arrangement is employed, a nozzle-like passage appears between the tube and delta-winglet vortex generator. The fluid accelerates in the constricted passage and significantly delays the flow separation. Thus, the size of the wake zone and form-drag is significantly decreased. Consequently, the addition of the delta winglet not only generates a longitudinal vortex, but also forms a nozzle-like acceleration zone that decreased the size of the wake zone behind the tube.

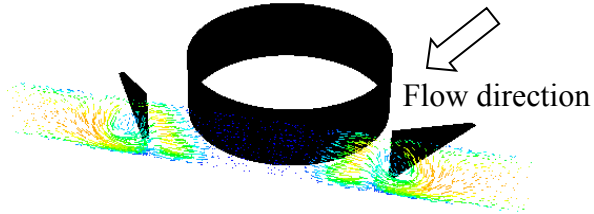


Fig. 7 Structure of longitudinal vortex ( $Re = 1000$ ) [31]

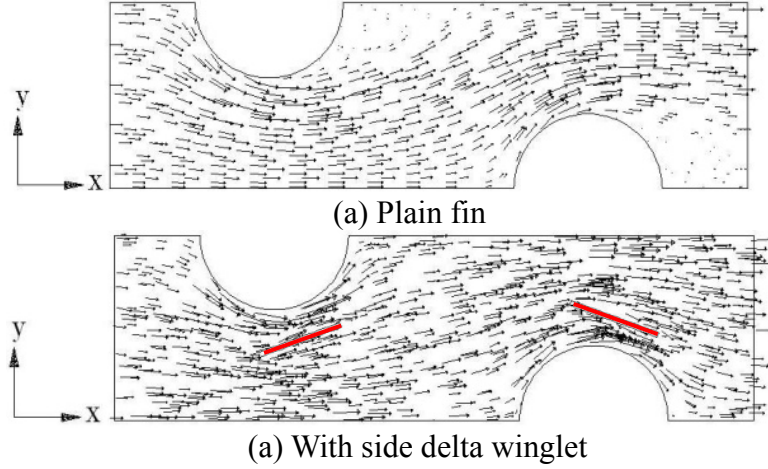


Fig. 8 Velocity vector plots on a plane near the fin ( $Re = 1000$ ) [31]

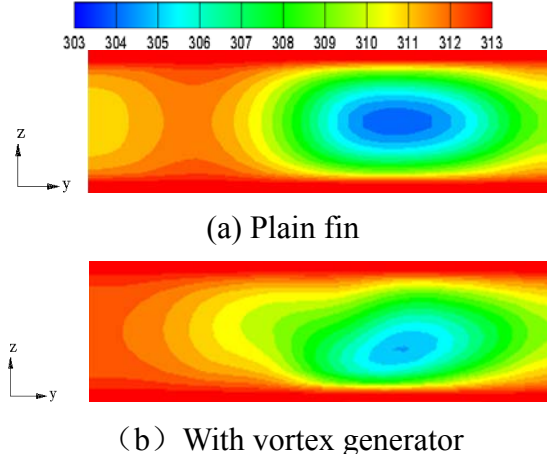


Fig. 9 Exit temperature distribution (K) [31]

Figure 9 shows the exit temperature distributions for plain fin and fin with delta winglets at  $Re = 1000$ . It can be seen that the exit temperature for the case of plain fin is vertically symmetric with respect to the middle-plane, but asymmetric for the case with vortex generator because the swirling flow rearranged the temperature distribution in the fluid. The air temperature gradient on the side with vortex generator is increased and the exit air temperature is higher than the case of plain fin. In other words, the difference between the air temperatures at inlet and outlet is increased. Consequently, the heat transfer rate with vortex generator is higher than the case of plain fin. Figure 10 shows the distribution of fin surface temperature for plain fin and fin with delta winglet at  $Re = 1000$ . It can be seen that the temperature gradient in the region behind the tube for the case with vortex generator is higher than the case of plain fin without vortex generator. At the same location, the local temperature for the case with the vortex generator is lower than that of the plain fin. The average fin temperature is also lower due to the addition of vortex generators. Thus, the delta winglet increases the heat transfer rate and consequently increases the overall heat transfer coefficient so that the heat transfer performance is improved.

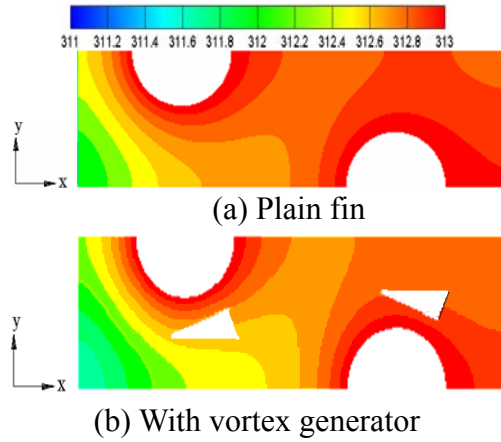


Fig. 10 Fin surface temperature distribution (K)

## (2) Effects of configuration and size of side delta winglet on the performance of fin-and-tube heat exchanger

The effects of tube arrangement, angle of attack and aspect ratio of delta winglets on the heat transfer performance and pressure drop of will now be analyzed.

The tubes in the fin-and-tube heat exchangers can be arranged either inline or staggered. Figure 11 shows the variation of Colburn factor,  $j$ , as function of Reynolds number for different arrangements. At the same Reynolds number, the Colburn factor for the case with vortex generators is higher than that of the plain fin, regardless the arrangements. The mechanisms of heat transfer enhancement can be explained by the fact that the delta winglet generates a secondary flow which allows the fluid to directly impinge to the fin surface. The boundary layer becomes thinner and the hot and cold fluids more vigorously mixed. In addition, there exists an accelerated zone between the side delta winglet, tube wall, and fin, which allows the fluid to enter the poorly ventilated region behind the tube and reduces the size of the wake zone.

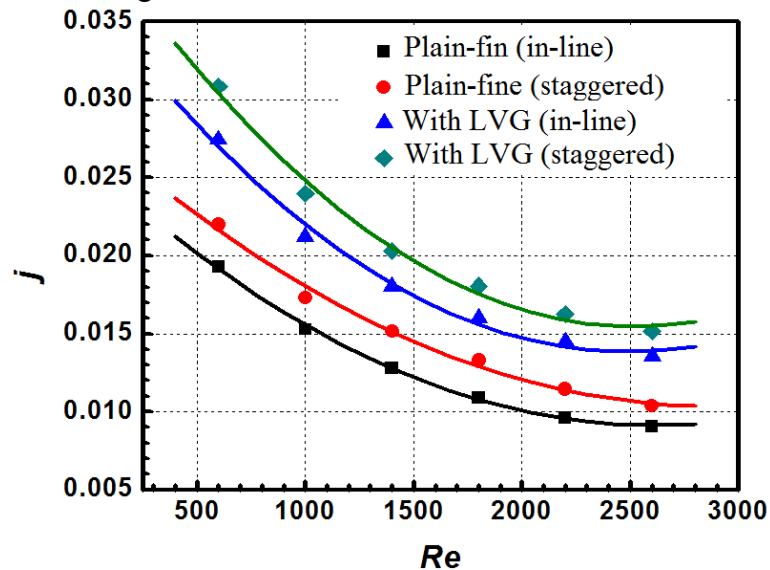


Fig. 11 Colburn factor vs. Reynolds number

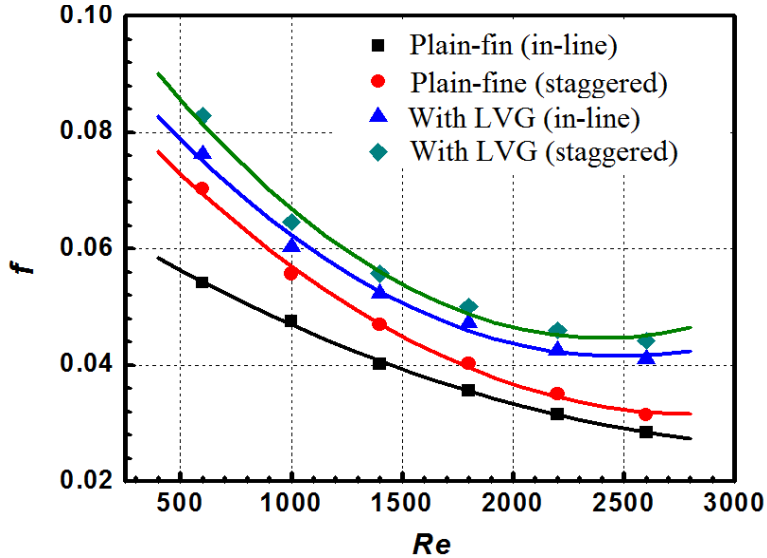


Fig. 12 Fraction factor vs. Reynolds number

In the range of Reynolds number that was studied, the heat transfer for inline arranged fin-and-tube heat transfer is enhanced by 38.8–50.9%, while the heat transfer enhancement for the staggered arrangement is 35.1–45.2%. In other words, the heat transfer enhancement for inline arrangement is better than that for the staggered arrangement.

Figure 12 shows the variation of fraction factor with Reynolds number for different arrangements. It can be seen that the friction factor decreases with increasing Reynolds number, and friction factor for the case with the vortex generator exhibits higher drag than that for the plain fin. For the fin-and-tube heat exchanger with side delta winglet, the change of the drag comes from two sources. First, the form drag of the delta winglet causes an increase of drag. On the other hand, the delta winglet on the side of the tube resulted in increase of the fluid velocity near the tube and delayed the boundary layer separation; the size of the wake region is decreased so that the form drag of the tube is decreased. In the range of Reynolds numbers studied, the friction factor for inline arranged fin-and-tube heat transfer is increased by 30.3% – 46.8%, while the increase of friction factor for staggered arrangement is 19.3% – 34.5%. It can also be seen from Fig. 12 that increase of friction factor due to delta winglet at higher Reynolds number is more significant than that at the low Reynolds number.

The ratios of Colburn factors to friction factors,  $j/f$ , for different tube arrangements are shown in Fig. 13. For both inline and staggered arrangements, the overall performances for the cases with delta winglets are better than those of the plain fins. This finding indicates that the enhancement of heat transfer is more significant than increase of the friction factor. It should be noted that as Reynolds number increases, increases of  $j/f$  due to delta winglet becomes less significant since increases of the friction factors at higher Reynolds numbers is more significant than at low Reynolds number. Therefore, it can be concluded that the delta winglet is more effective on enhancing heat transfer at low Reynolds numbers.

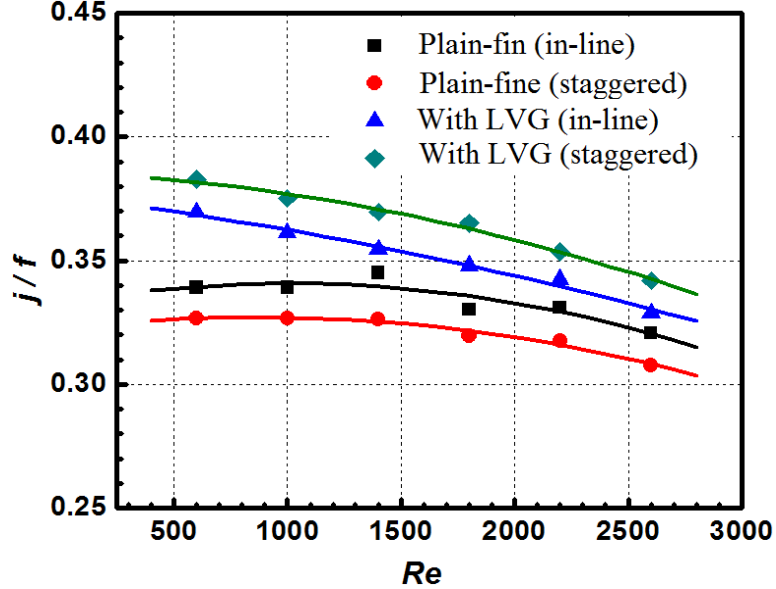


Fig. 13 Overall heat transfer and drag for different arrangements

In order to reveal the effects of angle of attack of the delta winglets on heat transfer and pressure drop, performance of fin-and-tube heat exchangers with delta winglets at five different angles of attack ( $\alpha = 10^\circ, 20^\circ, 30^\circ, 40^\circ$ , and  $50^\circ$ ) were studied. Figure 14 shows the Coburn factor versus Reynolds at five different angles of attack. It can be seen that heat transfer is enhanced for all five cases. For an unchanging Reynolds number, the Colburn factor increases with increasing angle of attack. Increases of the Coburn factor with angle of attack is more significant at small angle of attack, and such increases becomes less significant at large angle of attack. Figure 15 shows friction factor versus Reynolds number at different angles of attack. It can be seen that friction factor is increased for all five cases and the friction factor increases with increasing angle of attack. Increases of friction factor with angle of attack are less significant at small angle of attack. As angle of attack further increases, the increase of friction factor becomes more significant.

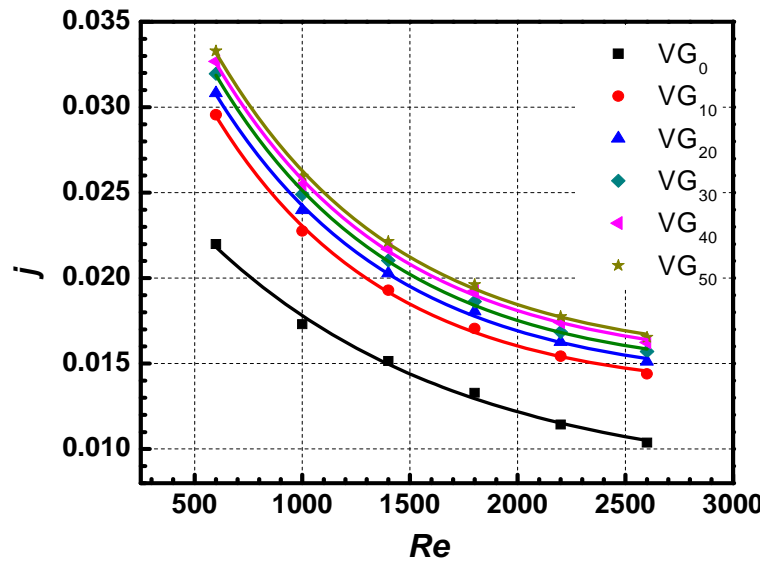


Fig. 14 Colburn factor vs. Reynolds number at different angles of attack [31]

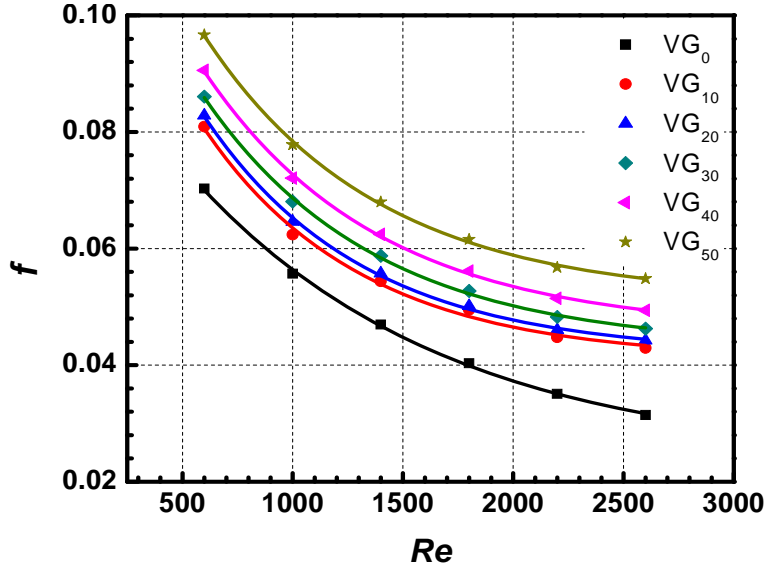


Fig. 15 Friction factor vs. Reynolds number at different angles of attack [31]

The relative heat transfer-to-drag performances for delta winglets at different  $s$  of attack are shown in Fig. 16. For the case that the angle of attack is  $50^\circ$ , the value of  $j/f$  is greater than the case of plain fin when the Reynolds number is under 1800. When the Reynolds number is above 1800, the  $j/f$  value for the case of delta winglet is lower than that of plain fin. For all other four angles of attack, the overall performances of the cases with delta winglet are better than that of the plain fin for all Reynolds numbers studied. It should be noted that the increase of  $j/f$  with increasing attack angle becomes less significant as Reynolds number increases. Therefore, side delta winglet type LVG is more effective at low Reynolds number. The computational results also indicate that among all structures studied, the delta winglet with angle of attack of  $20^\circ$  has the best overall performance.

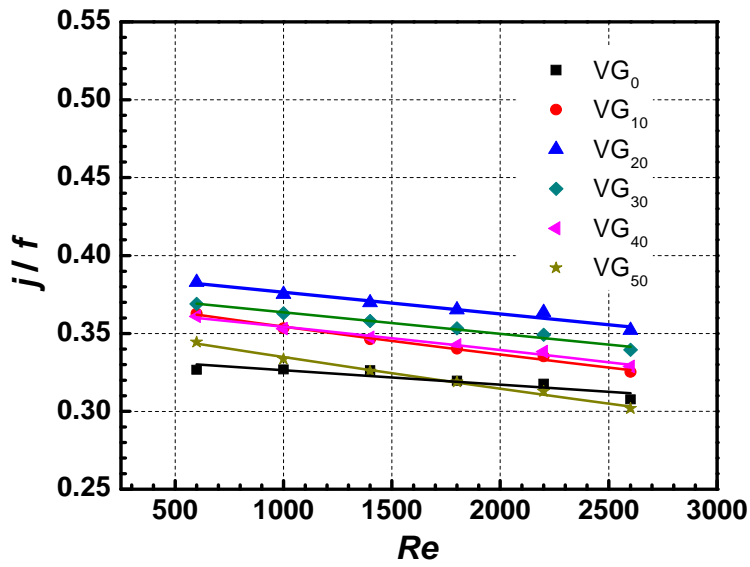


Fig. 16 Overall performances of heat transfer and drag at different angles of attack [31]

The effects of aspect ratio of the delta winglet are studied while the angle of attack is fixed at  $20^\circ$ . Figure 17 shows the Colburn factor versus Reynolds at different aspect ratios,  $\Lambda$ . Under a fixed Reynolds number, the Colburn factor increases with increasing aspect ratio, and the increase becomes less significant at higher aspect ratio. Figure 18 shows the friction factor versus Reynolds number at different aspect ratios. The friction factor increases with increasing aspect ratio and the increase becomes more pronounced at higher aspect ratio. The overall performances of heat exchanger with delta winglets at different aspect ratios are shown in Fig. 19. For all four aspect ratios that were studied, the value of  $j/f$  decreases with increasing Reynolds number. The delta winglets with aspect ratio of 2 have the best relative performance of heat transfer to pressure drop.

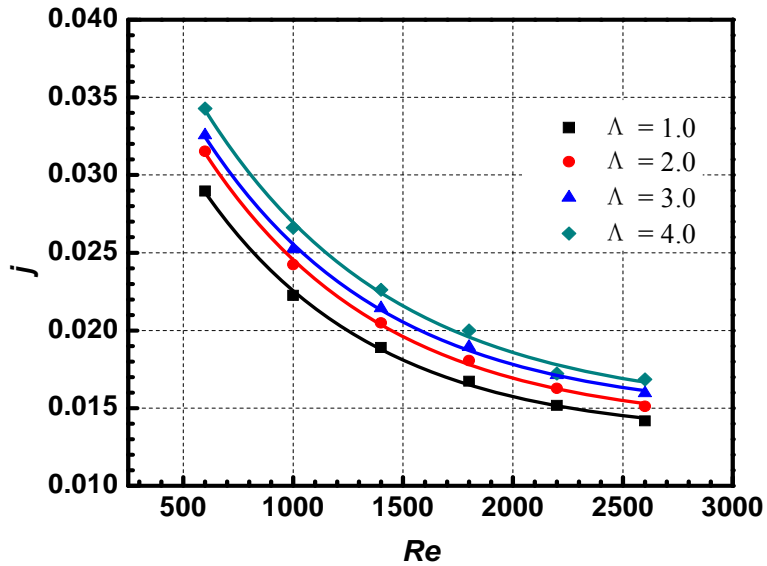


Fig. 17 Colburn factor vs. Reynolds number at different aspect ratios [31]

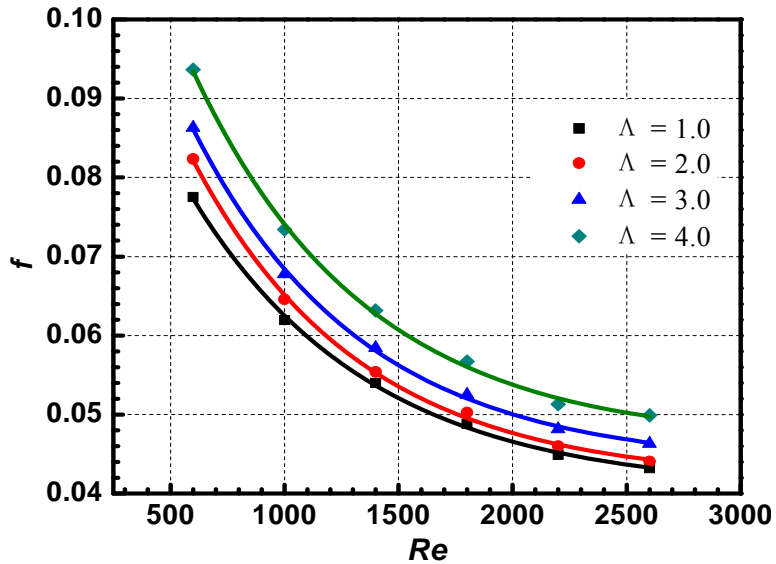


Fig. 18 Friction factor vs. Reynolds number at different aspect ratios [31]

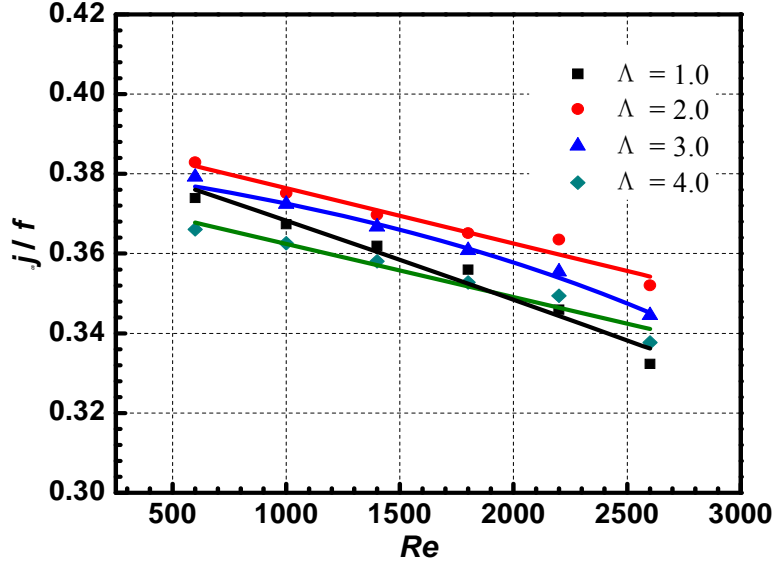


Fig. 19 Overall performances of heat transfer to drag at different aspect ratios

### 3.2.2 Application of LVGs in Wavy Fin-and-Tube Heat Exchangers

Combining LVGs with other heat transfer enhancement techniques can further improve the air-side heat transfer of the fin-and-tube heat exchangers. Sanders and Thole<sup>[32]</sup> experimentally studied the effects of winglets to augment tube wall heat transfer in louvered fin heat exchangers. The effects of the LVG's angle of attack, aspect ratio, direction, and shape on the performance of the fin-and-tube heat exchanger were investigated for  $230 < Re < 1016$ . For optimized winglet parameters, tube wall heat transfer augmentations as high as 39% were achieved with associated friction factor augmentations as high as 23%. Combination of LVGs with wavy fin-and-tube heat exchangers has received scant attentions in the past and was studied by our group [33-34]. The flow and heat transfer characteristics of wavy fin-and-tube heat exchangers as shown in Fig. 20 was investigated. Effects of angle of attack, number of rows, and wavy angle on the performance of the wavy fin-and tube heat exchangers were discussed.

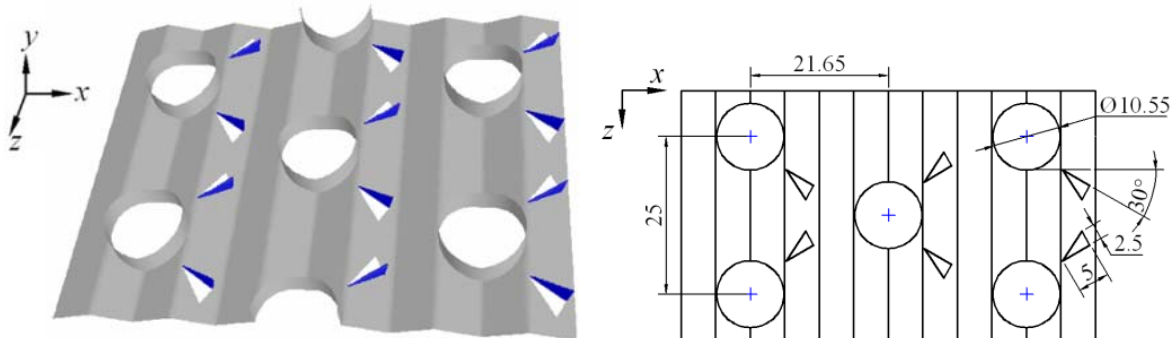


Fig. 20 Schematic of wavy fin with delta winglet [34]

#### (1) Effects of tube arrangements on flow and heat transfer

Figure 21 shows the variation of the cross-sectional average pressure along the air flow direction for the wavy fin with delta winglets in staggered and in-line arrays for Reynolds number (based on outer tube diameter) of 3000. The cross-sectional average pressure at any axial location is determined by the area-weighted average static pressure at this cross-section. There exists a steep

pressure drop near the tube. For the wavy fin with delta winglets, the cross-sectional average pressure has a slight drop at the axial location of the delta winglet, which is due to a small form drag induced by the slender delta winglet. The increase in the pressure drop penalty induced by the delta winglet is relatively small as indicated by Fig. 21.

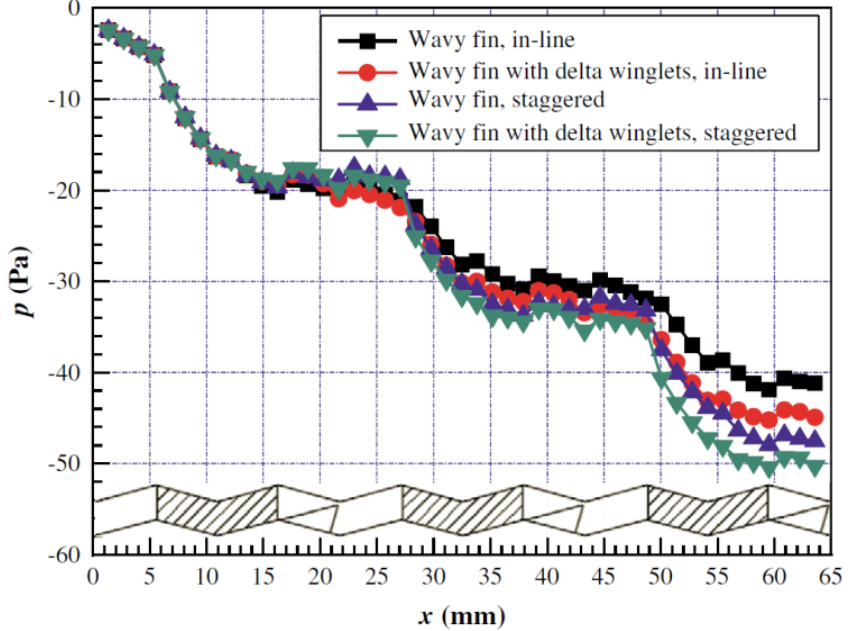


Fig. 21 Cross-sectional average pressure in the air flow direction [34]

Figure 22 shows effects of longitudinal vortices generated by delta winglets on the cross-sectional average heat transfer coefficient in the main flow direction. At the leading edges of fins of both inline and staggered arrangements, the heat transfer coefficient is the highest. However, the heat transfer weakens rapidly as boundary layer thickens. For the case of inline arrangement without a delta winglet, there exists large wake zones between tube rows where the heat flux is low. After delta winglets are added, the longitudinal vortices generated by delta winglets significantly enhance heat transfer in the zone between tube rows, which is evidenced by a peak of heat transfer coefficient between the tube rows. For the case of staggered tube arrangement without delta winglets, it is different from the inline arrangement in that fluid directly impinges on the tubes. The heat flux reaches to peak value at the stagnant point of every tube and then decreases as the boundary layer develops. Similar to the case of inline arrangement, there also exists a large wake zone behind every tube where heat transfer lessens. For the case with delta winglets, longitudinal vortices are generated, the wake zone becomes smaller, and the local heat transfer is significantly enhanced. It is evidence from Fig. 22(b) that a new heat flux peak appeared behind the tube due to longitudinal vortices. Therefore, for both inline and staggered arrangement, the longitudinal vortices generated by delta winglets significantly enhanced heat transfer in the wake zone which compensate the heat transfer in this poorest region in the fin-and-tube heat exchangers.

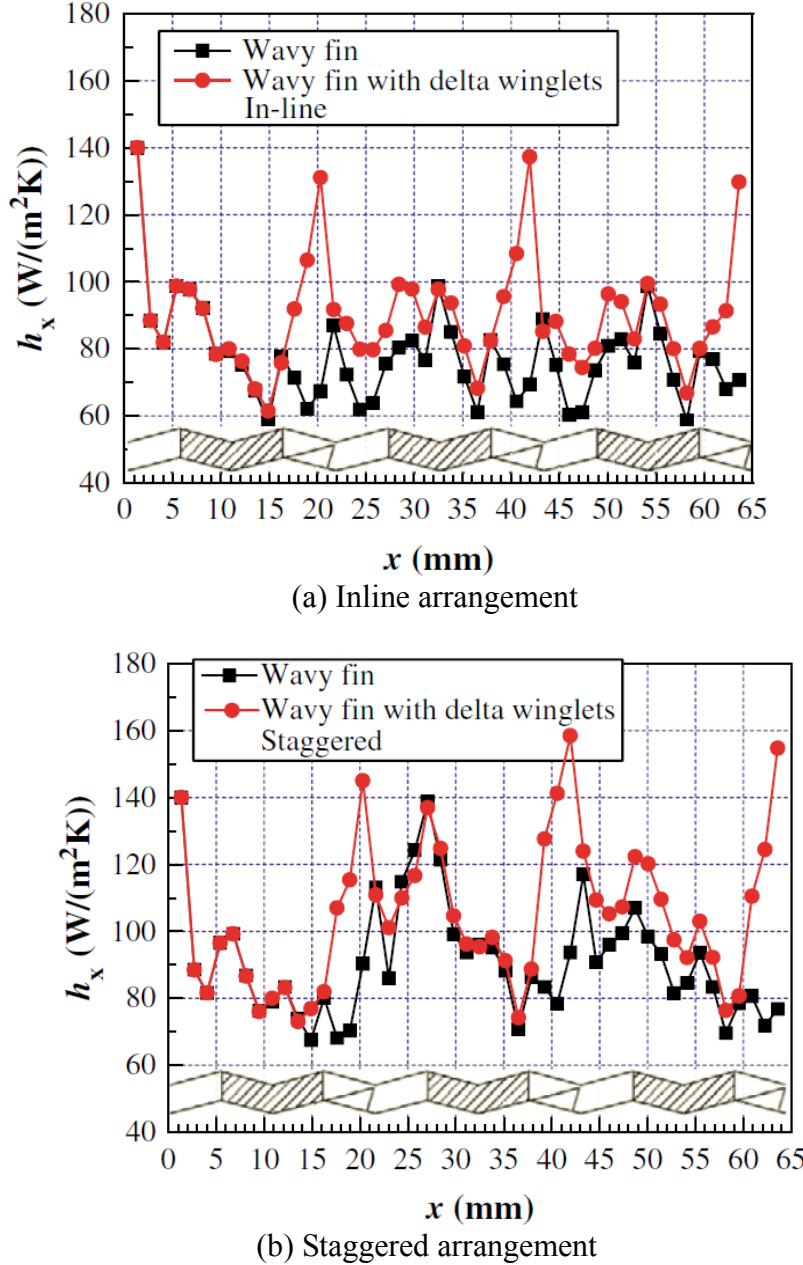


Fig. 22 Distribution of cross-sectional averaged heat transfer coefficient along the streamwise direction [34]

### (2) Effect of angle of attack of LVG on flow and heat transfer

Effects of angle of attack of the delta winglet on flow and heat transfer are investigated and compared to the cases with the same wavy fin-and-tube heat exchanger without LVGs. Figure 23 shows variations of Colburn factors and friction factors with Reynolds number at different angles of attack. It can be seen that both  $j$  and  $f$  for the case with delta winglets are greater than the case without delta winglets. Meanwhile, both  $j$  and  $f$  increase with increasing angle of attack  $\alpha$ . In the range of Reynolds numbers studied, the Colburn factor for the case with delta winglets and angle of attack of  $\alpha = 30^\circ$  is 8–12% higher than the case without delta winglets, while the friction

factor is only increased by 2–7%. At an angle of attack of  $\alpha = 45^\circ$ , the Colburn factor and friction factor are respectively increased by 13–17% and 9–12% after addition of delta winglets. When the angle of attack is further increased to  $\alpha = 60^\circ$ , the delta winglets resulted in increases of Colburn factor and friction factor by 17–21% and 19–21%, respectively. As the angle of attack increases, the projected area of the delta winglets normal to the incoming flow increases so that the form drag also increases. Meanwhile, the intensities of the longitudinal vortices also increases and their disturbances on flow are also stronger. As a result, both the heat transfer and the pressure drop increases with increasing angle of attack.

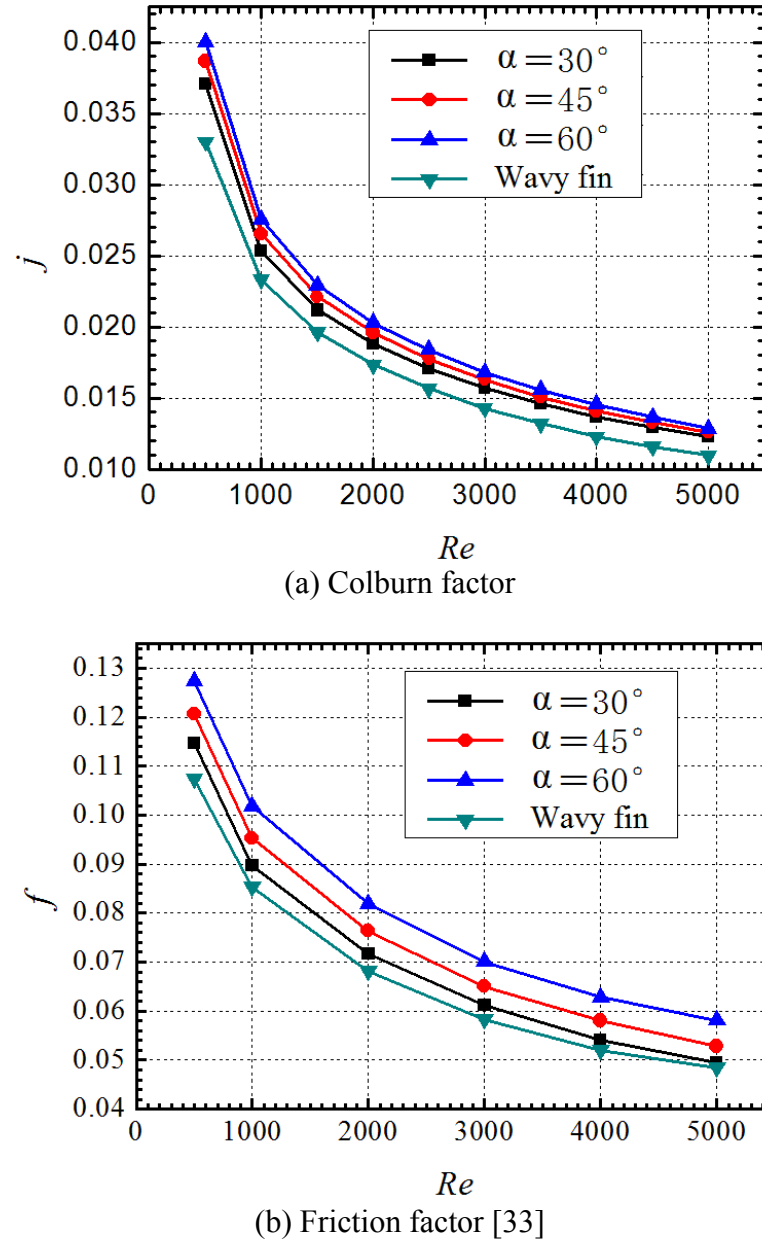


Fig. 23 Effects of angle of attack on Colburn factor and friction factor

Figure 24 shows the relative performance of the wavy fin-and-tube heat exchanger versus angle of attack  $\alpha$ . At the angle of attack of  $30^\circ$  and  $45^\circ$ , the ratio of Colburn factor and friction factor for the case with delta winglets are higher than the case without LVG;  $j/f$  is the largest at  $30^\circ$ . At angle of attack of  $60^\circ$ , on the other hand,  $j/f$  for the case with delta winglets is lower than that of the case without LVG for most Reynolds number except  $Re = 500$ . Therefore, at smaller angle of attack, the enhancement of heat transfer by LVGs is higher than the increase of the friction factor. As angle of attack increases, the cost of pressure drop outweighs the benefit of heat transfer enhancement.

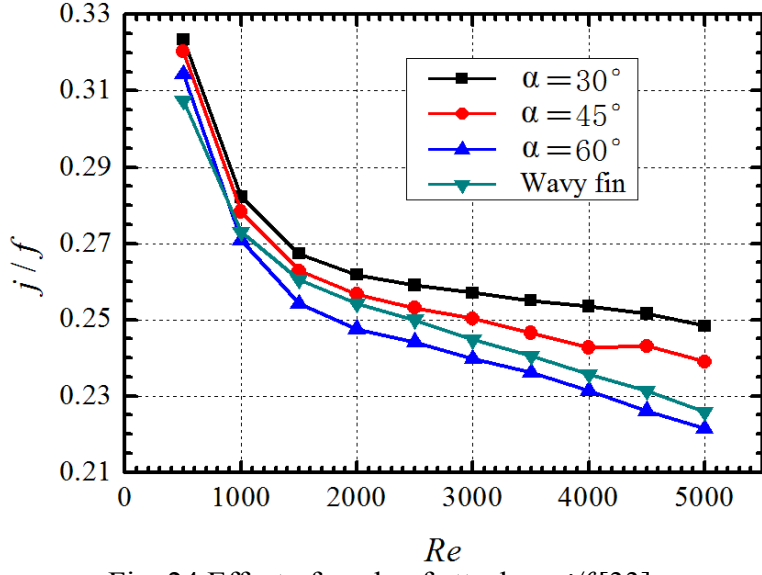
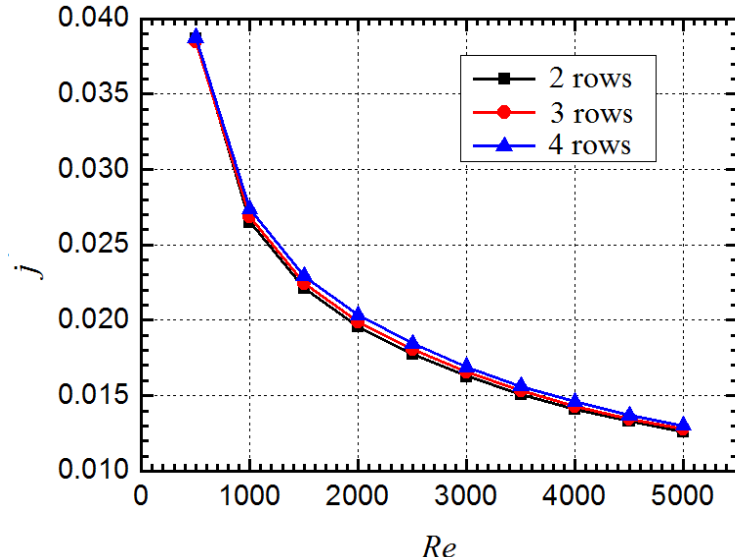


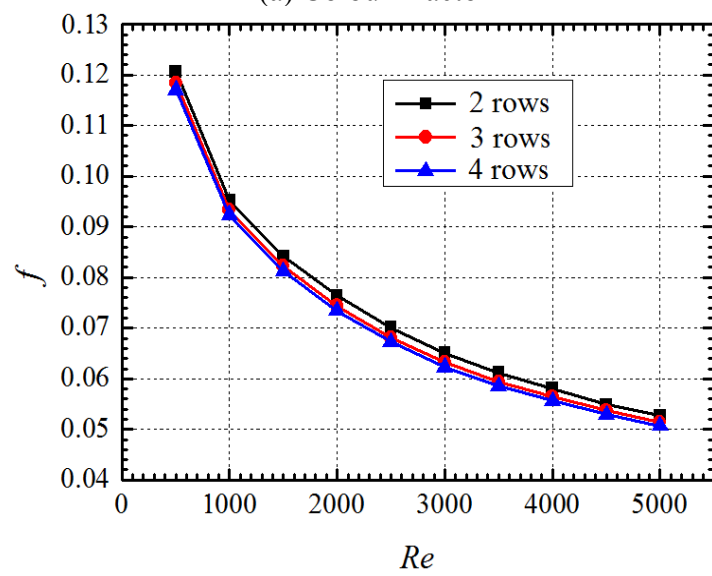
Fig. 24 Effect of angle of attack on  $j/f$  [33]

### (3) Effect of number of rows on flow and heat transfer

Effects of number of rows on flow and heat transfer in a wavy fin-and-tube heat exchanger with delta winglets are investigated. Figure 25 shows the variations of Colburn factors and friction factors with Reynolds number for different numbers of rows. The Colburn factor of the wavy fin-and-tube heat exchanger with delta winglets and four rows of tubes is slightly larger than that with two and three rows of tubes; the difference between the cases of two and three rows of tubes is very insignificant. The friction factor of the wavy fin-and-tube heat exchanger with delta winglets and two rows of tubes is slightly larger than that with three and four rows of tubes. Therefore, increasing number of rows results in slight increases of  $j$  and decreases of  $f$ . One can conclude that due to combined wavy and delta winglets, the disturbance in the channel causes the flow and heat transfer becomes fully-developed. Consequently, the effect of the number of rows on flow and heat transfer is not very significant. Figure 26 shows the effect of number of row of tubes on  $j/f$ . It can be seen that, under the same Reynolds number,  $j/f$  increases with increasing number of rows.



(a) Colburn factor



(b) Friction factor [33]

Fig. 25 Effects of the number of rows on Colburn factor and friction factor

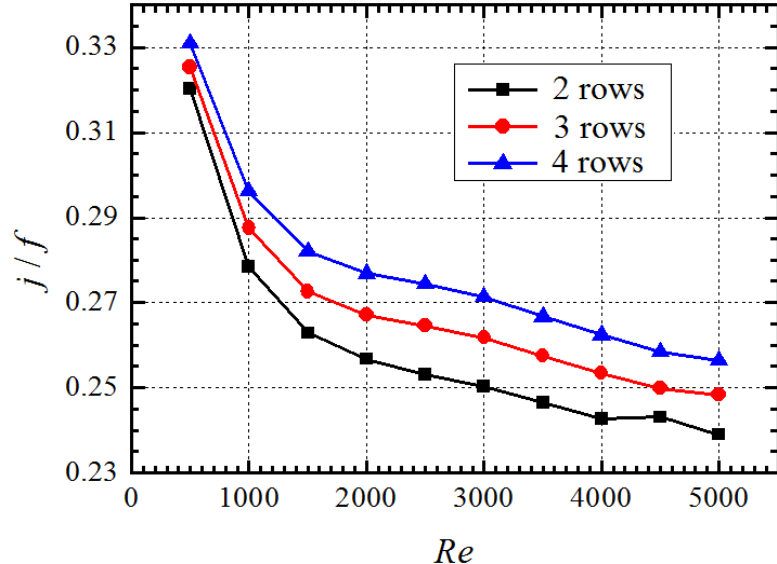
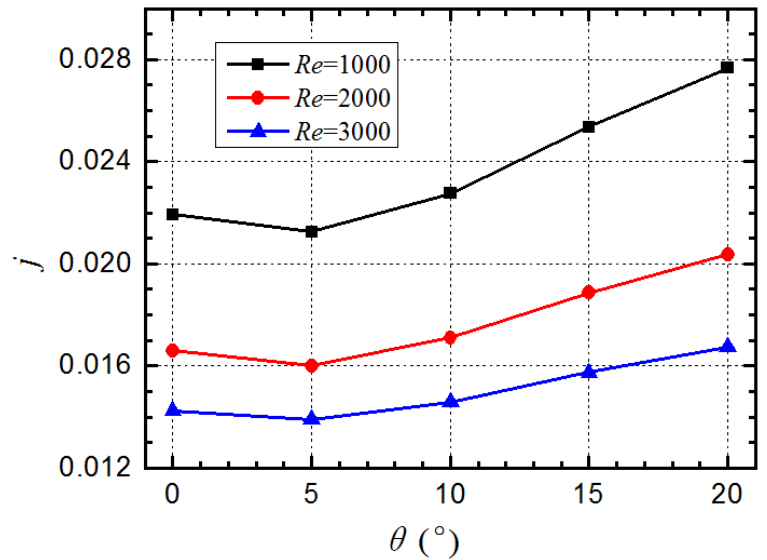


Fig. 26 Effect of number of rows on the overall performance [33]

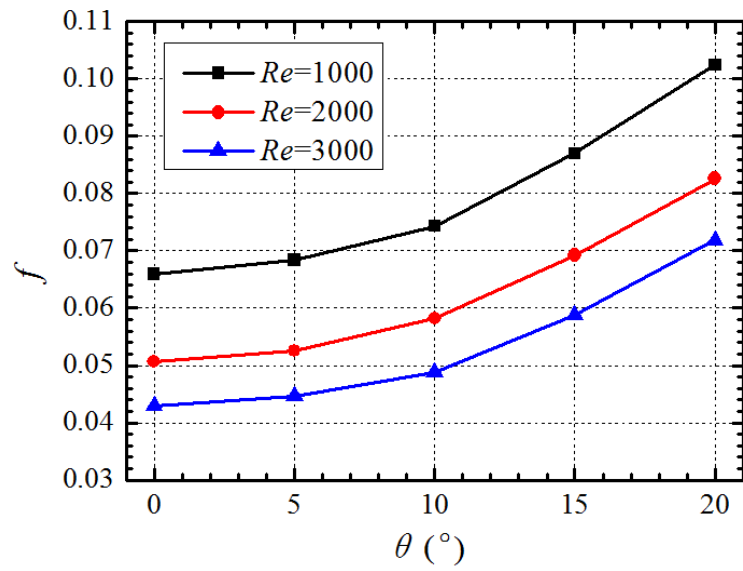
#### (4) Effect of wavy angle on flow and heat transfer

The flow and heat transfer at different wavy angles ( $\theta = 0^\circ, 5^\circ, 10^\circ, 15^\circ$ , and  $20^\circ$ ) are studied next. It should be pointed out that when  $\theta = 0^\circ$ , the wavy fin with LVGs becomes plain fin with LVGs. Figure 27 shows variation of  $j$  and  $f$  with Reynolds number at different wavy angles. As wavy angle increases, the Colburn factor decreases until  $\theta = 5^\circ$  and then increases afterwards, i.e., the heat transfer at  $\theta = 5^\circ$  is the poorest. When the wavy angle is increased to  $\theta = 10^\circ$ , the Colburn factor is slightly higher than the case of plain fin. The friction factor that reflects the flow characteristics increases with increasing wavy angle and the rate of increase becomes higher at larger wavy angle.

Figure 28 shows the effect of wavy angle on the overall performance of the heat exchanger. It can be seen that  $j/f$  decreases with increasing wavy angle. In other words, the increase of pressure drop due to increasing wavy angle is more significant than enhancement of heat transfer. Therefore, the relative performance of the fin degrades as wavy angle increases.



(a) Colburn factor



(b) Friction factor [33]

Fig. 27 Effects of wave angle on Colburn factor and friction factor

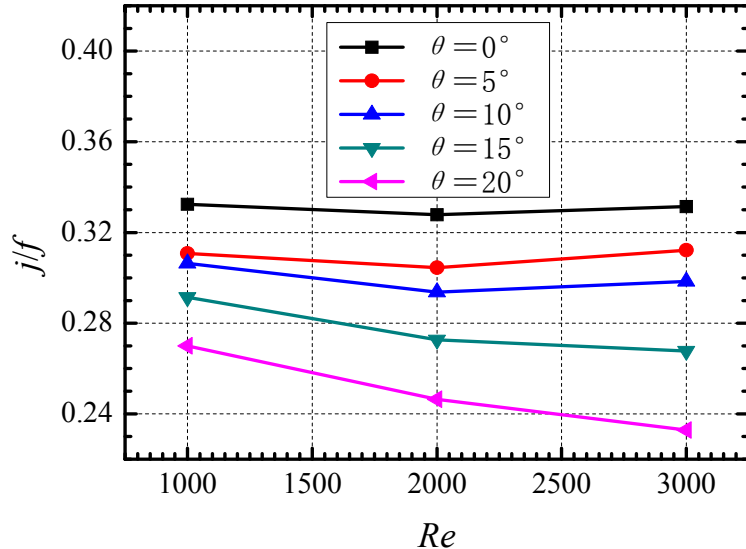


Fig. 28 Effect of wavy angle on the overall performance [33]

### 3.2.3 Applications of LVGs and oval tubes on fin-and-tube heat exchangers

Since the oval tube has better performance on drag reduction and can effectively decrease the size of the wake zone behind the tube, the pressure drop can be effectively decreased. On the other hand, LVGs increases the form drag in the channel and result in increases of drag and pressure drop. Therefore, combination of oval tube and LVGs can take advantages of both of these occurrences. The heat transfer capacity can be substantially increased without significant additional pressure losses.

Chen and Fiebig<sup>[35]</sup> numerically simulated fin-and-oval-tube heat exchangers with delta winglets. The angle of attack and aspect ratio of the delta winglet were optimized at  $Re = 300$ . Their results showed that the optimized overall heat transfer performance [ $(j/j_0)/(f/f_0) = 1.04$ ] can be obtained when the angle of attack was  $30^\circ$  and the aspect ratio was 2. Based on the above work, they thoroughly investigated the effect of multiple LVGs on the performance of heat exchangers with inline<sup>[36]</sup> and staggered<sup>[37]</sup> arrangements of tubes. Tiwari et al. <sup>[38]</sup> numerically studied performance of fin-and-oval-tube heat exchanger units with delta winglet and analyzed the flow and heat transfer under different numbers of LVGs (1–4 pairs) and arrangements (inline and staggered). Their results showed that the when two pairs of delta winglets are arranged inline, the average Nusselt number is increased by approximately 44%; when four pairs of delta winglets are staggered, the average Nusselt number is increased by about 100%.

O'Brien and Sohal <sup>[39]</sup> experimentally investigated flow and heat transfer in a narrow rectangular duct fitted with a circular tube and/or a delta-winglet pair. Their results showed that when a pair of delta winglets was installed, the average Nusselt number of the rectangular duct with fitted oval tubes was increased by 38%; while the corresponding drag was increased by 10% ( $Re_h = 500$ ) and 5% ( $Re_h = 5000$ ), respectively. Herpe et al. <sup>[40]</sup> numerically investigated the local entropy production rate of a finned oval tube with vortex generators. Their results showed that the volumetric entropy production rate is predominant in the strong flow gradient zones, which correspond to the outer surface of the longitudinal vortex and to the thinning zone of the boundary layer (down-wash zone).

The existing research has often focused on the performance of one type of heat transfer unit

(e.g., one oval tube), while the detailed studies on the flow and heat transfer of the entire channel are lacking. We investigated flow and heat transfer in fin-and-tube heat exchangers with delta winglets and the effects of key parameters are studied [41-43].

### (1) Effects of LVGs on flow and heat transfer in fin-and-oval-tube heat exchangers

In order to reveal the effects of LVGs on the overall flow and heat transfer performance of fin-and-tube heat exchangers, numerical simulations on fin-and-oval-tube heat exchangers with and without LVGs are performed. Figure 29 shows the schematic diagram of the fin-and-oval-tube heat exchangers with delta winglets. The LVGs are symmetrically installed behind the oval tubes and the shaded area is the computational domain. The flow channels of the fin-and-oval-tube heat exchangers without and with delta winglets are shown in Fig. 30. The locations and orientation of the LVGs are shown in Fig. 31. At the fin surface, non-slip and impermeable conditions are applied for velocities, while periodic conditions are applied for temperature.

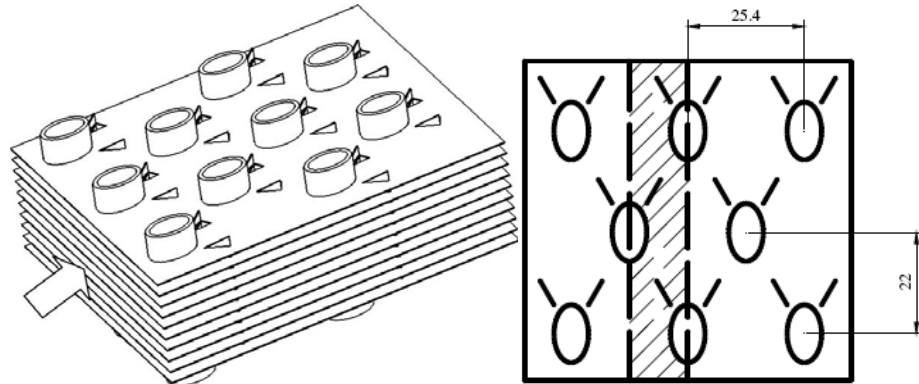


Fig. 29 Fin-and-oval tube heat exchangers with LVGs and the computational domain (unit: mm) [43]

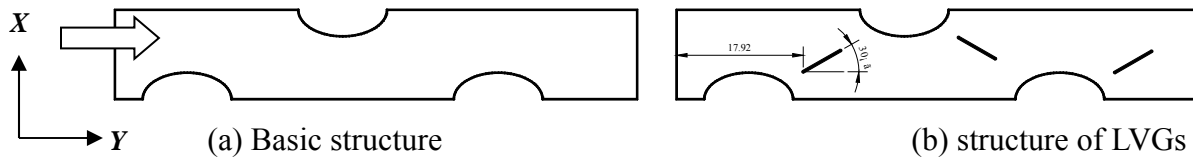


Fig. 30 Flow channel of the fin-and-oval-tube heat exchangers [43]

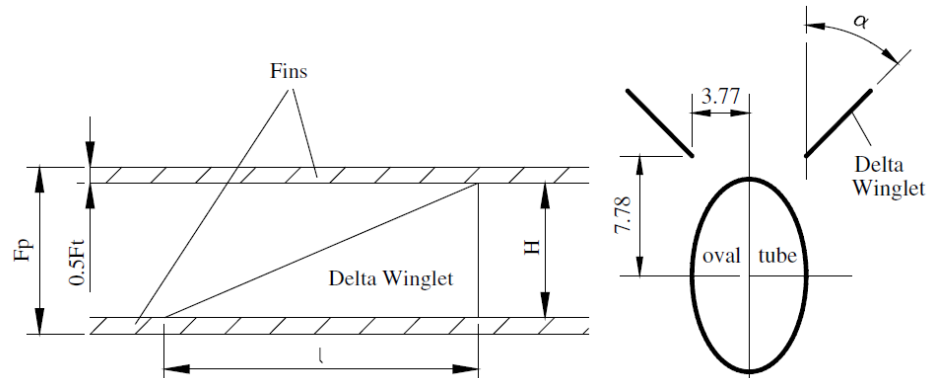


Fig. 31 Size and locations of the LVGs [43]

When air flows through the channel of the fin-and-oval-tube heat exchanger with LVGs, longitudinal vortices are generated due to the pressure difference before and after LVGs and the friction. The axis of this strong swirling secondary flow is same as the main flow direction. Due to strong disturbance of the LVGs, the boundary layers can be weakened or their formation can be interrupted. The strong funnel effects of the longitudinal vortices can also bring the fluid from the wake region to the main flow region. The cold fluid near the edge and the hot fluid in the main flow region can be well mixed and the heat transfer can be enhanced.

Figure 32 shows the isovel distributions in three  $x-z$  planes at  $Re = 1500$ . The velocity in the entrance region before LVGs is nearly uniform and without any vortices. After the fluid passes the LVGs, the generation of longitudinal vortices results in highly non-uniform isovels and produces a strong secondary flow. The transverse velocity can be as high as three times of the inlet velocity. The strong swirling flow transports the fluid near the fin and the tube wall to the core of main flow. Meanwhile, the fluid in the core of the main flow is also carried over to the region near fin and tube wall. These processes significantly promote mixing of hot and cold fluids and increase the heat transfer coefficient.

Figure 33 shows the velocity vector plots and streamlines at three cross-sections normal to the main flow direction. When the fluid passes the LVGs, the pressure variation and the separation of the fluid at the LVG surface generate very complex swirling flow. As can be seen from Fig. 33, in addition to the main vortex, induced vortices and corner vortices can also be formed. The combined effects from various vortices resulted in complete disturbance of the thermal boundary layer. The hot and cold fluids are fully mixed and heat transfer is enhanced.

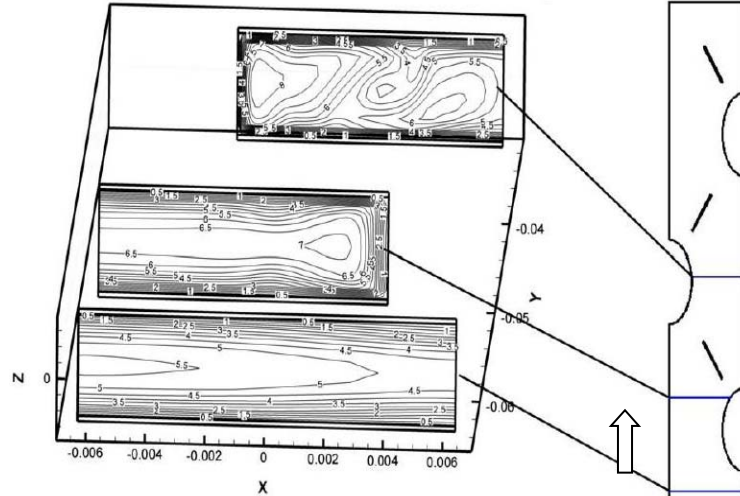


Fig. 32 Distributions of isovels in three cross-sections normal to the flow direction (unit: m/s)  
[43]

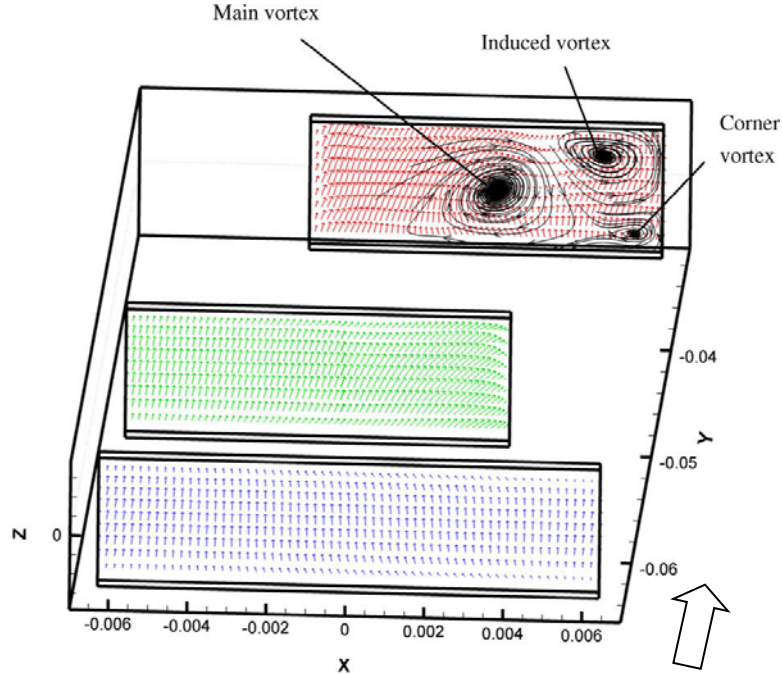


Fig. 33 Vector-plots and streamlines generated by LVGs in three cross-sections normal to the main flow direction [43]

Figure 34 shows the temperature contour at three cross-sections normal to the main flow at  $Re = 1500$ . In the entrance region, the isotherms are parallel to each other, and there is no apparent change on the thermal boundary layer before the fluid passing the LVGs. However, the isotherms are twisted and distorted after the LVGs. The thermal boundary layer becomes thinner and temperature gradient increases on the fin surface impinged by the longitudinal vortices. These changes increase the heat transfer coefficient on the fin surface and the heat transfer performance of the heat exchanger is improved.

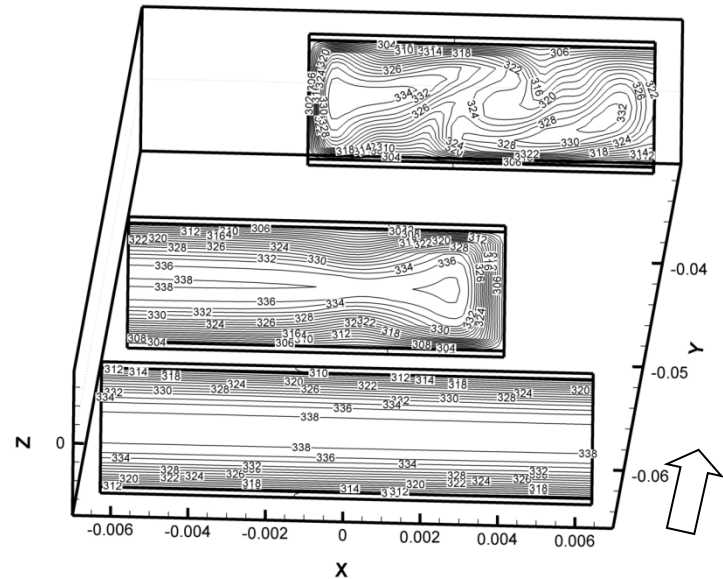


Fig. 34 Isotherms on three cross-sections of the normal to the main flow direction (unit: K) [43]

Figure 35 shows the local velocity distribution on a mid-plane that is parallel to the x-y plane for the cases without and with LVGs. It can be seen from Fig. 35(a) that there exists a large wake zone for the case without LVGs. The fluid in this zone is almost isolated from the fluid in the main flow. A thermal barrier is formed and heat transfer in this zone is extremely poor. After the LVGs are installed, the strong transverse secondary flow generated from the longitudinal vortices effectively reduces the size of the wake zone. Meanwhile, the fluid with high momentum is redirected to the oval tube surface by the longitudinal vortices, which, in turn, effectively delays the separation of boundary layer on the oval tube (see Fig. 35(b)). All of the above mechanisms can effectively contribute to the enhancement of heat transfer. In the figures, the flow direction is from bottom to top.

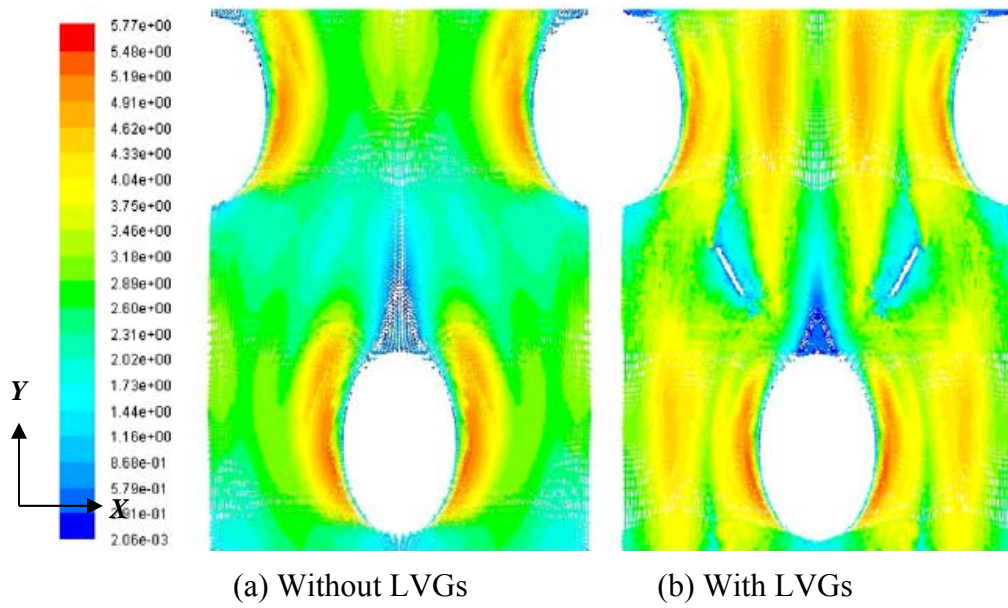


Fig. 35 Local velocity distribution on the middle cross-section (unit: m/s) [43]

Figure 36 shows the local temperature profiles on the middle cross-section for  $Re = 1500$ . It can be seen from Fig. 36(a) that the temperature in the aforementioned thermal barrier zone is close to that of the oval tube. The thermal barrier zone becomes significantly smaller after LVGs are installed (see Fig. 36(b)). Comparison of Fig. 36(a) and (b) indicates the temperature distributions before LVGs are almost the same for both cases. However, the fluid temperature is significantly lowered after the fluid passing LVGs, especially in the downstream region of the LVGs. The generation of the longitudinal vortices altered the flow field and promoted the mixing between the cold and hot fluids. The temperature gradient on the heat transfer surface is also increased, which ultimately resulted in heat transfer enhancement in the entire heat exchanger. As before, the flow direction is bottom to top.

Figure 37 shows the average Nusselt number versus Reynolds number for the case without and with LVGs. It can be seen that both Nusselt numbers increase with increasing Reynolds number. In the range of Reynolds numbers studied ( $Re = 500 - 2500$ ), the fin-and-oval-tube heat exchanger with LVGs showed better heat transfer performance over the case without LVGs. The use of LVGs increases the average Nusselt number by approximately 14-33%. Figure 38 shows the friction factor versus Reynolds number for the case without and with LVGs. Both friction factors decrease with increasing Reynolds number. In the range of Reynolds numbers studied ( $Re$

$= 500-2500$ ), the fin-and-oval-tube heat exchanger with LVGs exhibited higher friction factor over the case without LVGs. The increase in friction factor is approximately 30-41%. The reason for the increased friction factor is that the existences of LVGs increased the form drag so that the pressure drop for the heat exchanger is increased.

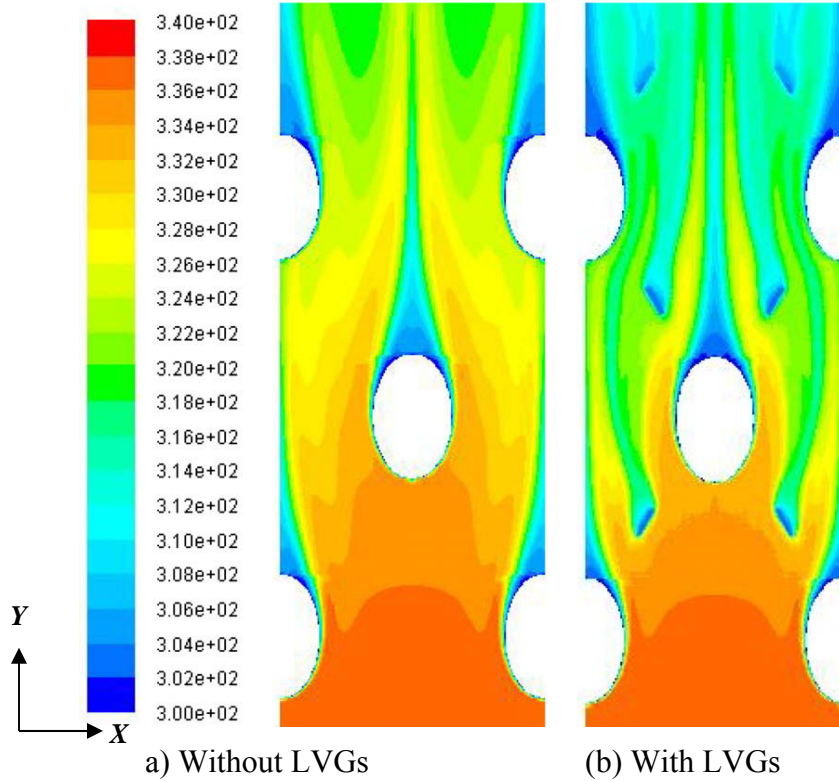


Fig. 36 Local temperature profiles on the middle cross-section (unit: K) [43]

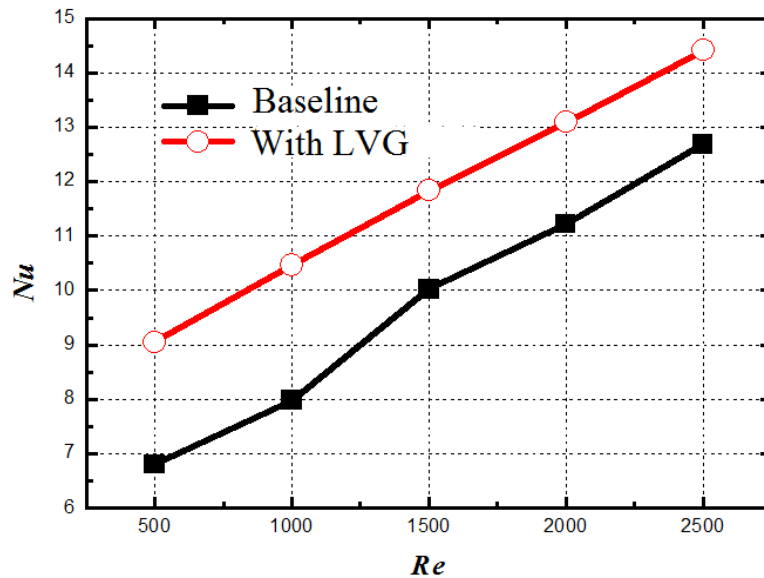


Fig. 37 Average Nusselt number versus Reynolds number for fin-and-oval-tube heat exchangers [43]

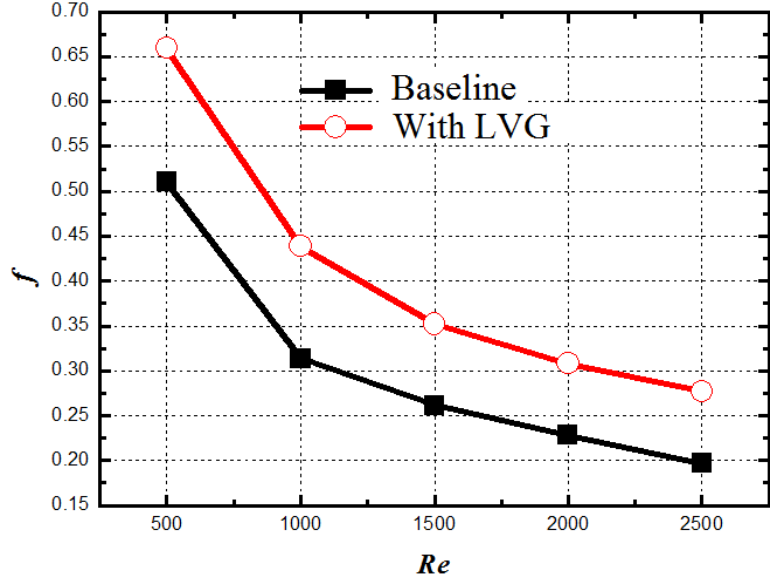


Fig. 38 Friction factor versus Reynolds number for fin-and-oval-tube heat exchangers [43]

The simulation results are also analyzed by using the field synergy principle [24], where the intersection angle between velocity and temperature gradient is an important parameter. Figure 39 shows the average interaction angle versus Reynolds number. It can be seen that the average intersection angles for both cases decrease with increasing Reynolds number. This means that as Reynolds number increases, the disturbance becomes stronger and the angle between velocity vector and temperature gradient decreases. In other words, the synergy between the velocity and temperature fields is improved. In the range of Reynolds numbers studied ( $Re = 500$ — $2500$ ), the intersection angle for the fin-and-oval-tube heat exchanger with LVGs is always less than that for the case without LVGs. This means that LVGs improve the synergy between velocity field and temperature in the heat exchanger and decrease the intersection angle, which leads to enhancement of heat transfer performance.

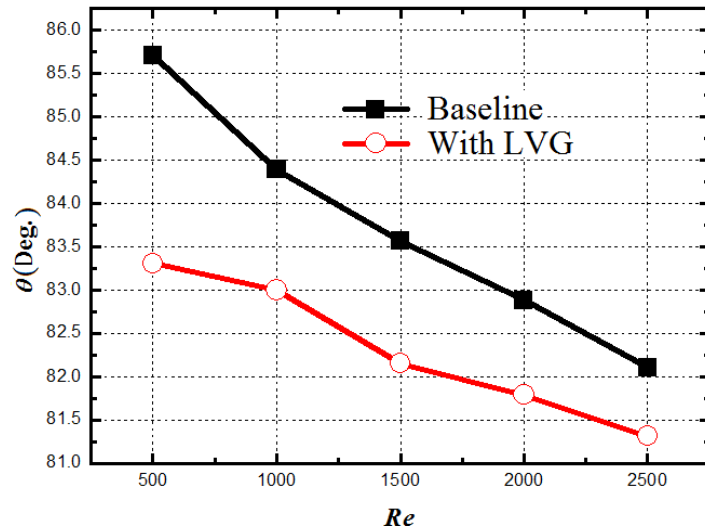


Fig. 39 Comparison of intersection angle between velocity vector and temperature gradient for fin-and-oval-tube heat exchangers [43]

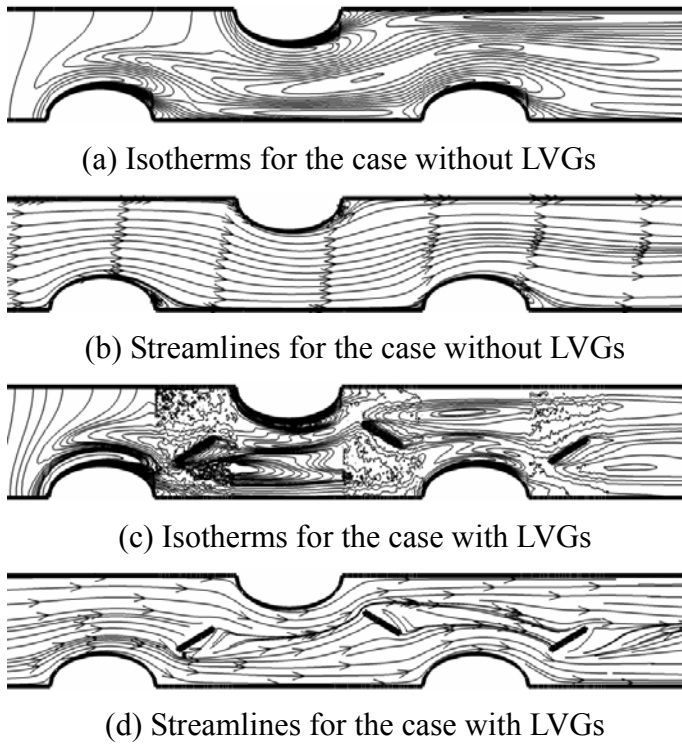


Fig. 40 Comparison of synergies between velocity and temperature fields for the case without and with LVGs [43]

In order to demonstrate the improvement of synergy between the flow field and temperature field, Fig. 40 shows comparison between the synergies between the flow and temperature fields for the cases without and with LVGs. Figure 40 (a) and (b) show the isotherms and streamlines for the case without LVGs. At the inlet of the heat exchanger, the isotherms and the streamlines are almost perpendicular to each other, which indicate that the synergy between the flow and temperature fields is very good. As flow continues to the wake zone, the isotherms are stretched and are parallel to the streamlines due to recirculation in the wake region. This means that the intersection angle between the velocity vector and the temperature gradient increases and the synergy between flow and temperature fields worsens. Figure 40 (c) and (d) show the isotherms and streamlines for the case with LVGs. Similar to the case without LVGs, the isotherms and the streamlines are almost perpendicular to each other at the inlet of the heat exchanger. As flow continues to the wake zone, the LVGs generated longitudinal vortices at the downstream of the oval tubes. The strong swirling secondary flow altered the local velocity and temperature fields so that the intersection angle between the velocity and isotherms is increased. In other words, the angle between the velocity and the temperature gradient is decreased and the synergy between velocity and temperature in the wake zone is improved and the overall heat transfer capacity of the heat exchanger is increased.

## (2) Effects of placements of the LVGs

In order to investigate the effects of locations of LVGs on the overall flow and heat transfer, the two structures shown in Fig. 41 are numerically investigated. The LVGs are either placed upper stream or downstream.

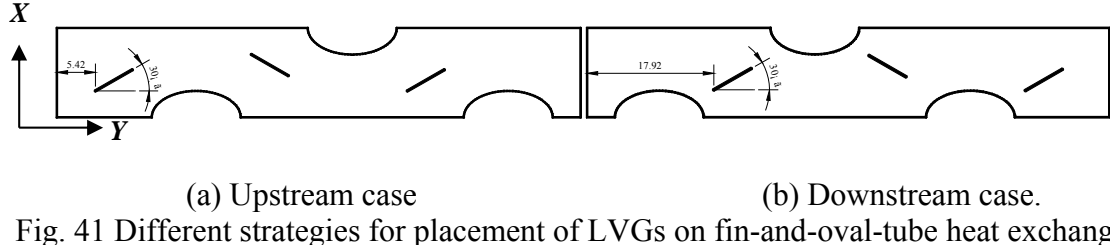


Fig. 41 Different strategies for placement of LVGs on fin-and-oval-tube heat exchangers [43]

Figure 42 shows the average Nusselt number versus Reynolds number for the two different structures. It can be seen that the Nusselt numbers for both cases increase with increasing Reynolds number. In the ranges of Reynolds numbers studied, the heat transfer performance for the downstream case is better than that of the upstream case. At the entrance of the heat exchangers, the heat transfer performance is very good due to the entry effects. The synergy between the velocity and temperature fields is also very good so that the potential of heat transfer enhancement at the entrance region is very small. On the other hand, placement of LVGs at the downstream can effectively take advantage of the entry effects and is helpful to reduce the size of the wake zone to enhance heat transfer. This is also in agreement of the principle of synergy for heat transfer, i.e., enhancing heat transfer in the zone where synergy is poor.

Figure 43 shows the friction factor versus Reynolds number for the two different structures. It can be seen that the friction factors for both cases decrease with increasing Reynolds number. Under the same Reynolds number, the friction factor for the upstream case is slightly lower than that of the downstream case.

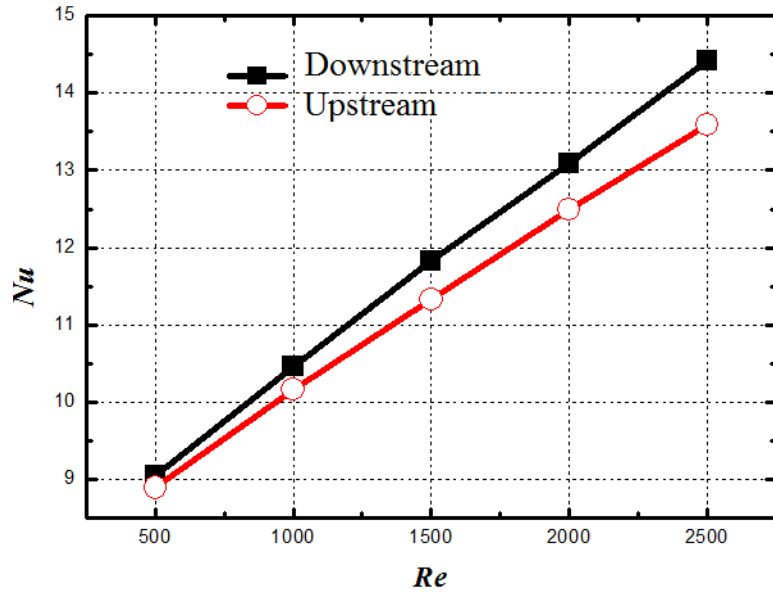


Fig. 42 Nusselt number vs. Reynolds number for different placements of LVGs in fin-and-oval-tube heat exchangers [43]

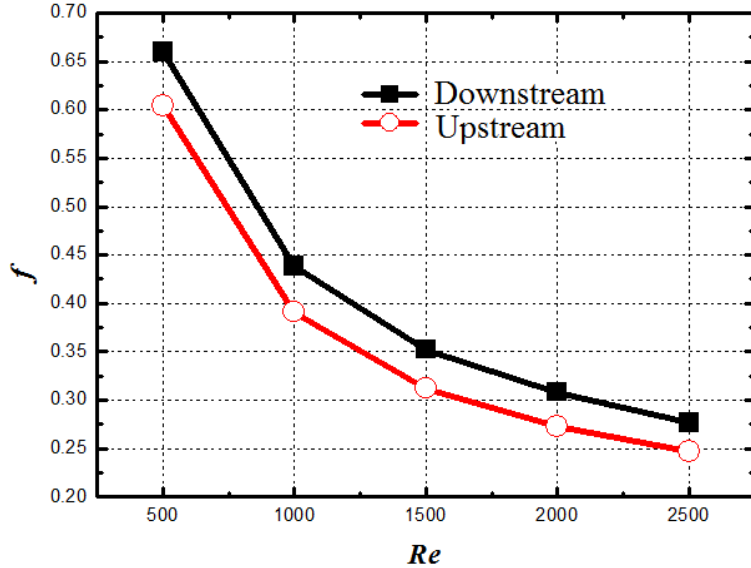


Fig. 43 Friction factor vs. Reynolds number for different placements of LVGs for fin-and-oval-tube heat exchangers [43]

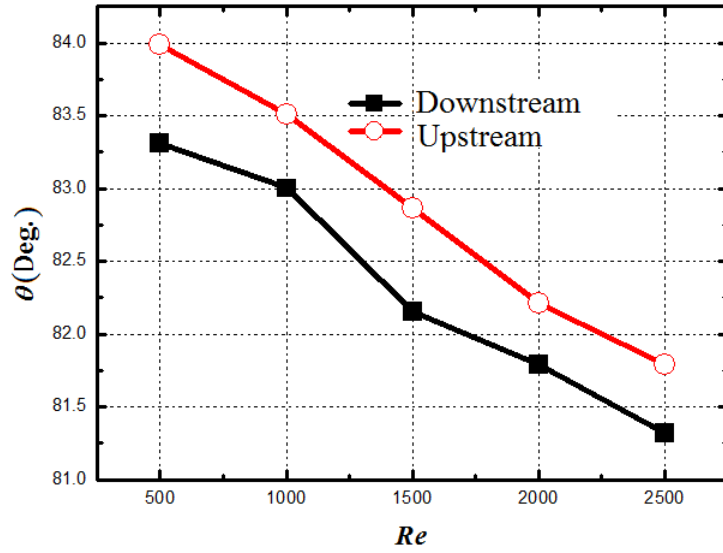


Fig. 44 Average intersection angle vs. Reynolds number for different placements of LVGs for fin-and-oval-tube heat exchangers [43]

Figure 44 shows the average intersection angle between velocity and temperature gradients versus Reynolds number for the two different structures. It can be seen that the placing the LVGs downstream can effectively improve the heat transfer in the wake zone where heat transfer is poorest and decrease the intersection angle. Consequently, heat transfer in the entire heat exchanger is enhanced.

In order to demonstrate variation of synergies between velocity and temperature fields for different LVG placements, Fig. 45 shows the isotherms and streamlines for the two different cases. The isotherms and streamlines for the upstream case are shown in Figs. 45 (a) and (b). As can be seen, the synergy at the entrance region is improved due to LVGs. However, the synergy

in the wake zone where heat transfer is poorest did not show much improvement. The isotherms and streamlines for downstream case are shown in Figs. 45 (c) and (d). The synergy at the entrance region is very good so that heat transfer enhancement in this region is not necessary. In the wake zone where heat transfer is poorest, the synergy is significantly improved, which, in turn, resulted in improvement of the heat transfer performance for the entire heat exchanger. Therefore, the downstream case is more helpful to improve heat transfer in the region where heat transfer is poorest and enhance heat transfer performance of the heat exchanger.

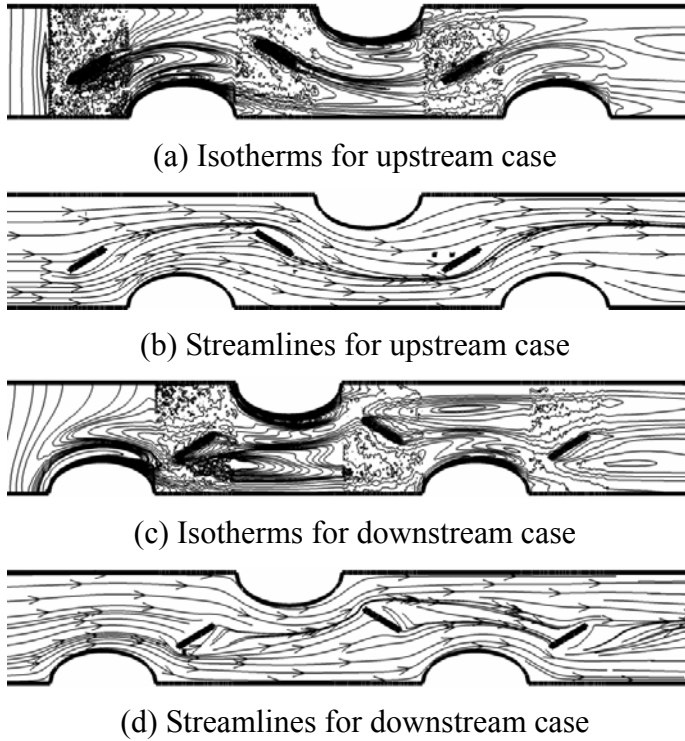


Fig. 45 Comparison between isotherms and streamlines for different placements of LVGs in fin-and-oval-tube heat exchangers [43]

### (3) Effects of angle of attack

The effects of angle of attack for the downstream case will now be investigated. The number of rows are  $n=3$  and the range of Reynolds number is  $Re = 500-2500$ . The heat transfer enhancements at the following angles of attack are studied:  $\alpha = 15^\circ, 30^\circ, 45^\circ$ , and  $60^\circ$  ( $0^\circ$  corresponds to the baseline case without LVGs).

Figure 46 shows the average Nusselt numbers of the heat exchanger with LVGs versus Reynolds number at different angles of attack. The effect of longitudinal vortices on heat transfer enhancement is not only dictated by the intensity of the vortices, but also depends on the persistency of the vortices. Both intensity and persistency of the longitudinal vortices are affected by the angle of attack  $\alpha$ . It can be seen from the figure that first the average Nusselt number increases with the increasing angle of attack  $\alpha$ , then the average Nusselt number reaches the maximum at the angle of attack of  $\alpha = 30^\circ$ , and decreases thereafter. When  $\alpha < 30^\circ$ , the intensities of the longitudinal vortices increase with increasing angle of attack; therefore, the average Nusselt number increases. In fact, the LVGs not only generate longitudinal vortices, but

also generate some transverse vortices, which can also enhance heat transfer. The transverse vortices can affect the persistency of the longitudinal vortices, or even destroy the longitudinal vortices. When  $\alpha > 30^\circ$ , although the intensity of the longitudinal vortices continuous to increase, the persistency of the longitudinal vortices is decreased due to effects of transverse vortices. Therefore, the results of heat transfer enhancement are affected and the average Nusselt number is slightly decreased. When the angles of attack continuous to increase beyond  $65^\circ$ , what the vortices generated by the LVGs are mainly transverse. Consequently, the effectiveness of LVGs on heat transfer enhancement is significantly affected.

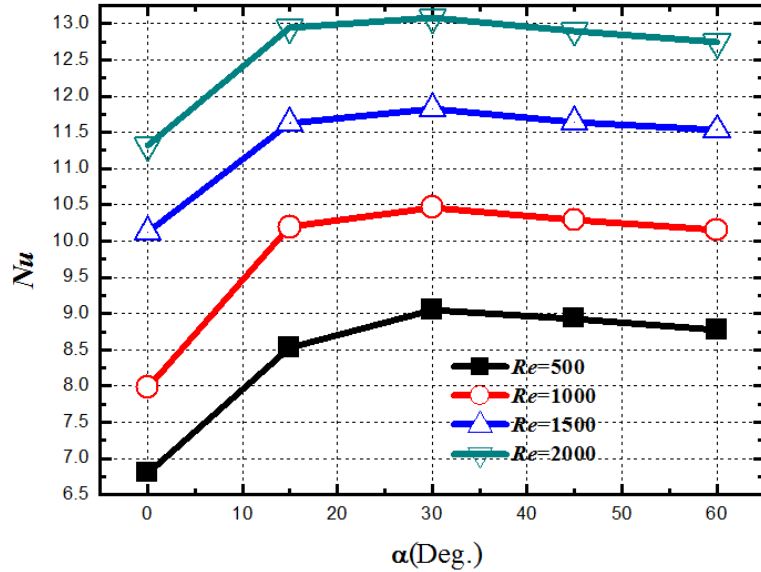


Fig. 46 Nusselt number vs. Reynolds number at different angle of attack for fin-and-oval-tube heat exchangers [43]

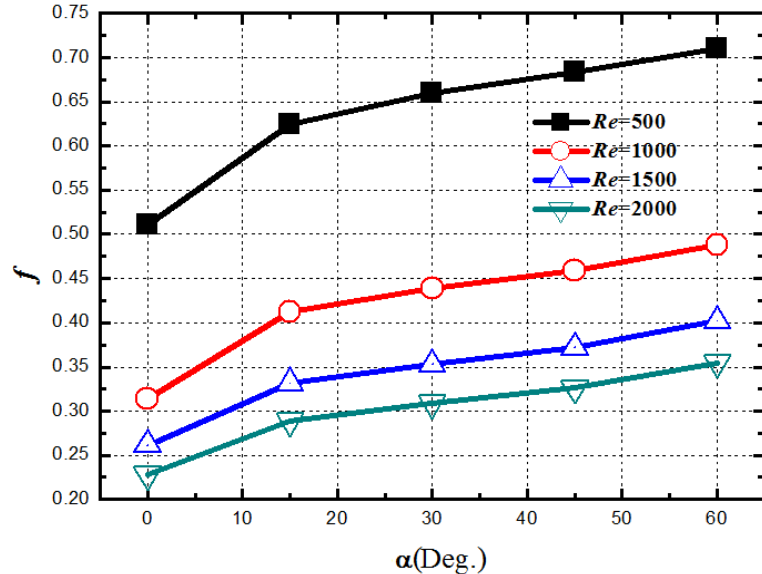


Fig. 47 Friction factor vs. Reynolds number at different angle of attack for fin-and-oval-tube heat exchangers [43]

Figure 47 shows the friction factor versus Reynolds number at different angles of attack. It can be seen that the friction factor increases with increasing angle of attack. As has already been identified earlier, as the angle of attack increases, the increasing form drag causes increased friction factor.

Figure 48 shows the comparison of synergies between velocity and temperature fields for the cases with angles of attack of  $30^\circ$  and  $60^\circ$ . At the entrances of the two heat exchangers and before the LVGs, the isotherms and streamlines for the two cases are almost the same: the streamlines and isotherms are almost perpendicular to each other, i.e., the synergies for both heat exchangers are very good. As the fluids pass the LVGs, the synergy between the temperature and velocity fields in the wake zone for the case with an angle of attack of  $30^\circ$  is significantly improved. On the contrary, the angle between the isotherms and streamlines in the wake zone for the case with an angle of attack of  $60^\circ$  is very small, and the isotherms and streamlines are even parallel in some region. Therefore, the synergy between the temperature and velocity fields is poor, and there is no significant improvement on synergy for the case of with an angle of attack of  $60^\circ$ .

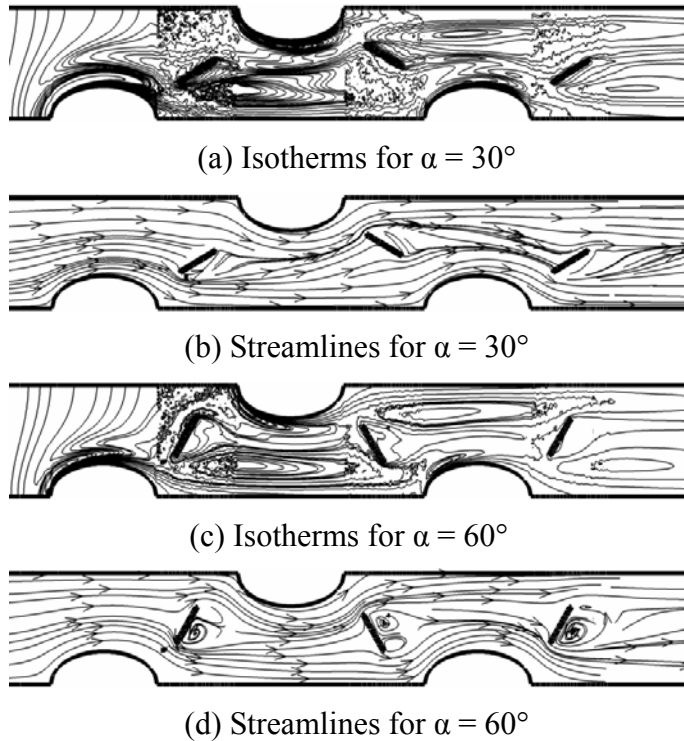


Fig. 48 Comparison of synergies between temperature and velocity fields at different angles of attack for fin-and-oval-tube heat exchangers [43]

#### (4) Effects of the number of rows of tubes

Based on the conclusion that the angle of attack of  $\alpha = 30^\circ$  can provide the best result on heat transfer enhancement, the effect of the number of rows on the performance of the fin-and-oval-tube heat exchanger with delta winglets is studied. The numbers of rows are 2, 3, 4 and 5, and the angle of attack of the downstream LVGs are  $30^\circ$ . The range of the Reynolds number is  $Re = 500-2500$ .

Figure 49 shows the average Nusselt number of the fin-and-oval-tube heat exchanger with LVGs versus the number of rows of tubes at different Reynolds numbers. It can be seen that the Nusselt numbers decrease with increasing number of rows of tubes, and trends for different Reynolds number are the same. The variations of the average Nusselt number from  $n = 2$  to  $n = 3$  is more significant than that from  $n = 3$  to  $n = 4$  or from  $n = 4$  to  $n = 5$ .

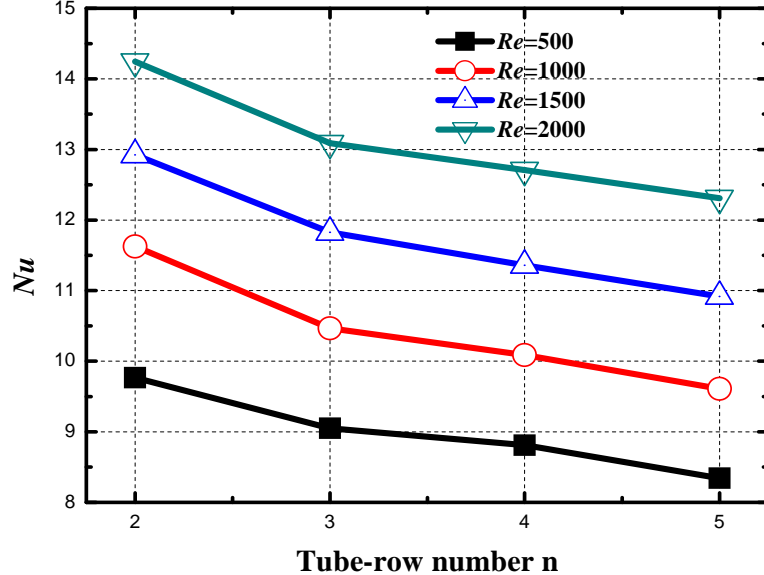


Fig. 49 Average Nusselt number vs. number of row of tubes for fin-and-oval-tube heat exchangers [43]

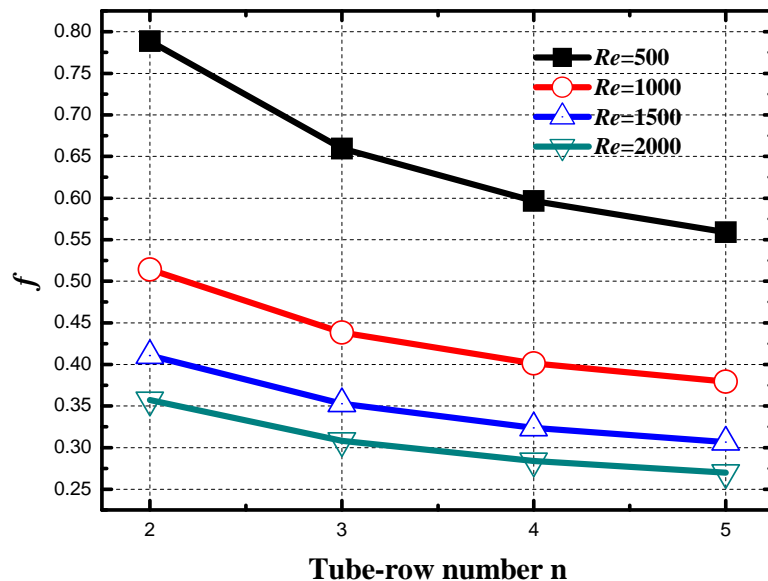


Fig. 50 Friction factor vs. number of row of tubes for fin-and-oval-tube heat exchangers [43]

Figure 50 shows the friction factors of the fin-and-oval-tube heat exchanger with LVGs versus the number of rows of tubes at different Reynolds numbers. It can be seen that the friction

factor decreases with increasing number of rows of tubes, and trends for different Reynolds numbers are similar to each other. The variations of the friction factors from  $n = 2$  to  $n = 3$  is more significant than that from  $n = 3$  to  $n = 4$ , which is, in turn, more significant than that from  $n = 4$  to  $n = 5$ . Thus, one can conclude that, as the number of rows increases, the effects of the number of rows on the average Nusselt number and friction factor become less significant.

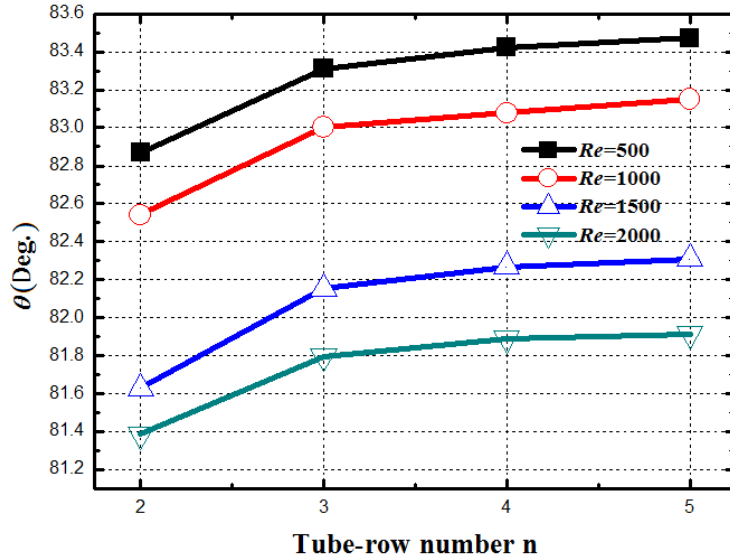


Fig. 51 Average interaction angle vs. number of row of tubes for fin-and-oval-tube heat exchangers [43]

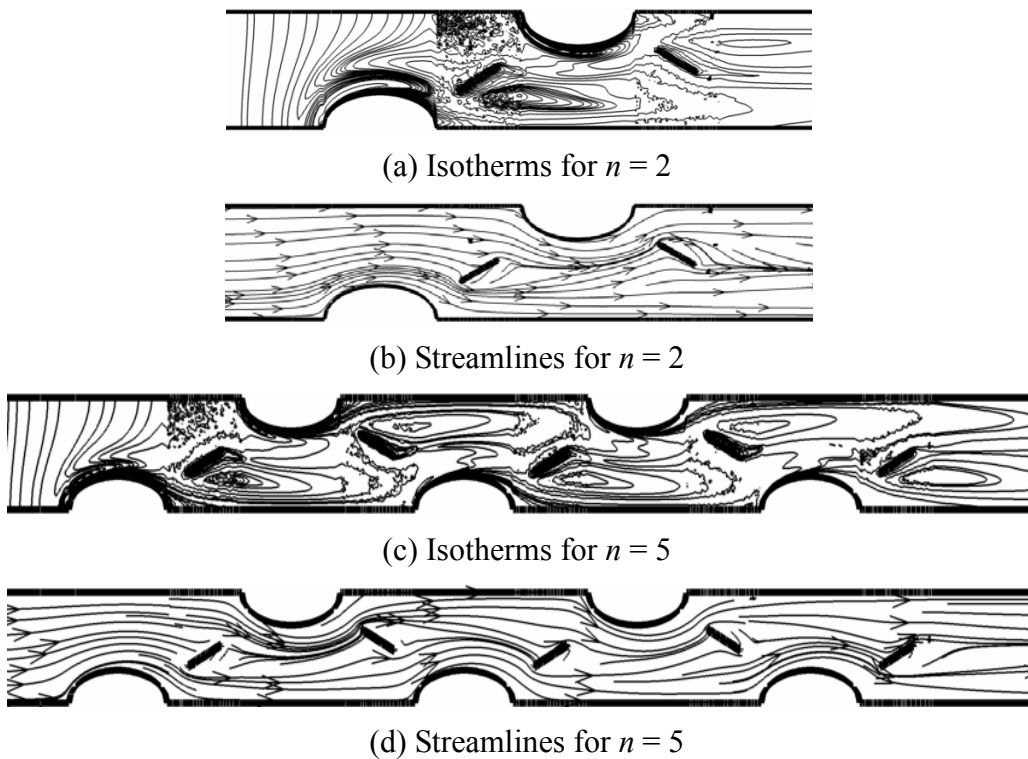


Fig. 52 Comparison for Synergies between temperature and velocity fields [43]

Figure 51 shows the average intersection angle between the temperature and velocity fields versus number of row of tubes at different Reynolds numbers. As the number of rows of tubes increases, the average intersection angle increases. The variations of the intersection angle from  $n = 2$  to  $n = 3$  is more significant than that from  $n = 3$  to  $n = 4$ , which is significant than that from  $n = 4$  to  $n = 5$ . In other words, the intersection angle increases with increasing number of row of tubes but the increase becomes less significant at large number of rows; this is consistent with the variation of Nusselt number shown in Fig. 49. The variations of intersection angle at different Reynolds numbers are similar to each other.

Figure 52 shows the comparison of synergies of temperature and velocity fields at different number of rows of tubes. At the entrances of the two heat exchangers, the isotherms and streamlines for both cases are almost perpendicular to each other, i.e., the synergies for both heat exchangers are very good. As for the isotherms and streamlines for the case of  $n = 5$ , the isotherms and streamlines before the second row are almost identical to case of  $n = 2$ . As the flow further develops, the isotherms for the case of  $n = 5$  gradually stretch and their angle with streamlines become smaller and smaller. In other words, the synergy between the temperature and velocity field becomes poorer and poorer. As a result, the synergy for the case of  $n = 5$  is worse than that of the case of  $n = 2$ .

### 3.2.4 Application of LVGs to fin-and-tube heat exchangers with multiple row of tubes

As mentioned earlier, the two most commonly reported LVG placement strategies are “common-flow-down” and the “common-flow-up” approaches <sup>[10]</sup>, which can be abbreviated as CFD and CFU approaches (see Fig. 53). Most existing research about heat transfer enhancement with LVGs deal with the CFD approach, while the research on flow and heat transfer in CFU approach is scant.

Under the CFD approach, the fluid between a pair of delta (or rectangular) winglet flows toward the fin with LVGs so that it is called flow *down*. CFD is characterized by the fact the distance between the heads of the delta winglets are longer than that between the tails. On the other hand, for the CFU approach, the fluid between a pair of delta (or rectangular) winglet flows away from the fin with LVGs so that it is called flow *up*. The distance between the heads of the delta winglets are shorter than that between the tails.

With regard to the studies on the heat transfer enhancement by LVGs with CFU placement, Joardar and Jacobi<sup>[10]</sup> numerically simulated fin-and-tube heat exchangers with 7 rows of tubes. They found that at  $Re = 850$ , heat transfer for the case of heat exchangers with 3 rows of tubes arranged inline and delta winglets is enhanced by approximately 32% and the corresponding friction factor is increased by 41%. They also obtained another interesting result that when the tube arrangement is changed to staggered, the same heat transfer enhancement can be obtained while the friction factor was only increased by about 33%. However, no explanation about the effect of tube arrangement on the friction factor was provided.

Joardar and Jacobi<sup>[44]</sup> performed experimental investigation for fin-and-tube heat exchanger with delta winglet. They found that when the Reynolds number was between 220-960, one row of delta winglets could increase heat transfer coefficient by 16.5-44% and the corresponding increase of friction factor was less than 12%. For the case of three rows of delta winglets, the heat transfer is enhanced by 29.9-68.8%, and the corresponding friction factor is increased by 26.0- 87.5%.

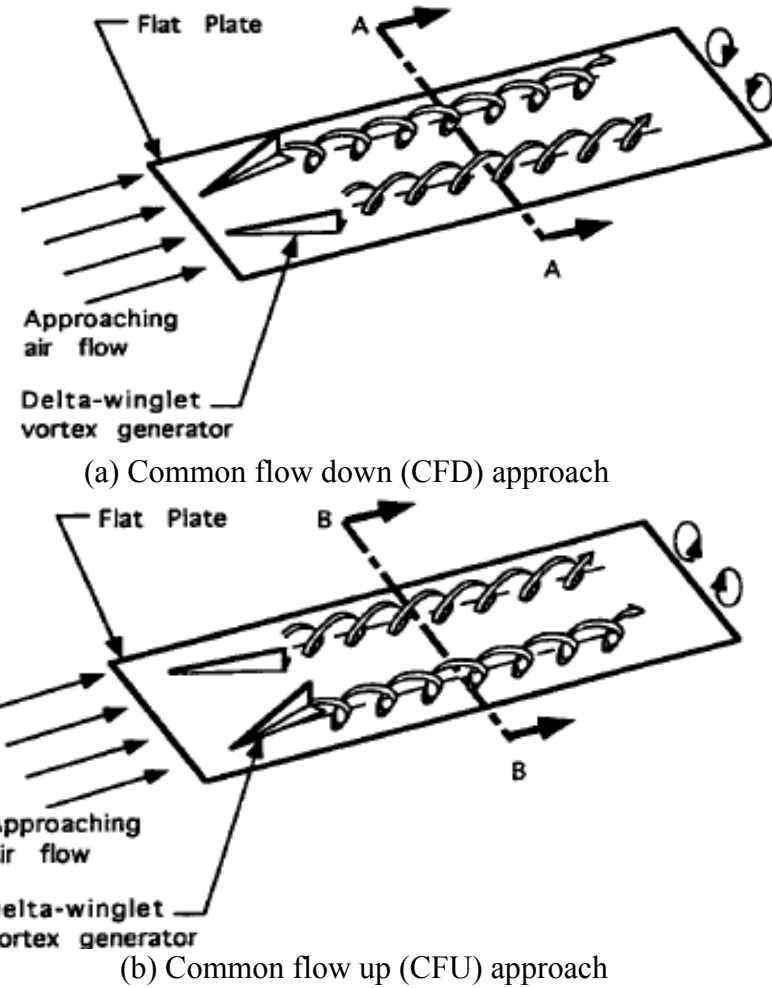


Fig. 53 Schematic of different placement strategies of LVGs [5]

Torri et al. [8] experimentally studied flow and heat transfer of fin-and-tube heat exchanger with only one row of delta winglets. For a staggered tube arrangement, the Colburn factor was increased by 10- 30%, while the friction factor,  $f$ , is decreased by 34-55%. For an inline arrangement, the Colburn factor was increased by 10- 20%, and the friction factor,  $f$ , was decreased by 8- 15 %. Kwak and Torri<sup>[9]</sup> studied flow and heat transfer of fin-and-tube heat exchangers with inline and staggered arrangements and one or two rows of delta winglets. They obtained the similar conclusion that the CFU placement of LVGs enhanced heat transfer while decreased drag.

Most existing research on LVGs with CFU placement used delta winglets while research on rectangular winglets is rare. The reason that the CFU placement has an advantage is that in addition to generating strong secondary swirling flow, a convergent flow channel can be formed between the LVG and the tube wall. The fluid is accelerated when it passes the convergent channel. This flow impinges on the tubes in the next row and thereby enhances heat transfer. This high-velocity impinging flow can also delay the separation of the boundary layer and reduce the size of the wake zone so that the form drag of the tube banks can also be reduced. When

rectangular winglets are employed, these advantages are more significant since more fluids are accelerated as they pass the convergent channel. We investigated the applications of rectangular winglets on enhancement of fin-and-tube heat exchangers and performed parametric studies [45, 46].

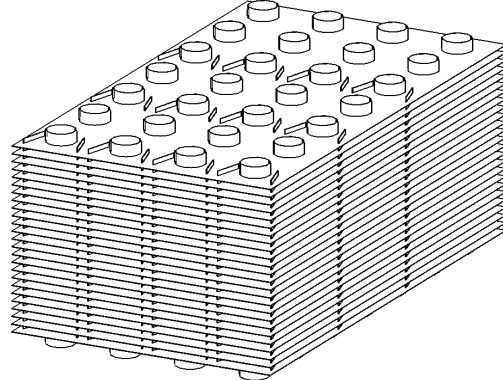


Fig. 54 Schematic of the core region of a fin-and-tube heat exchanger with rectangular winglets [46]

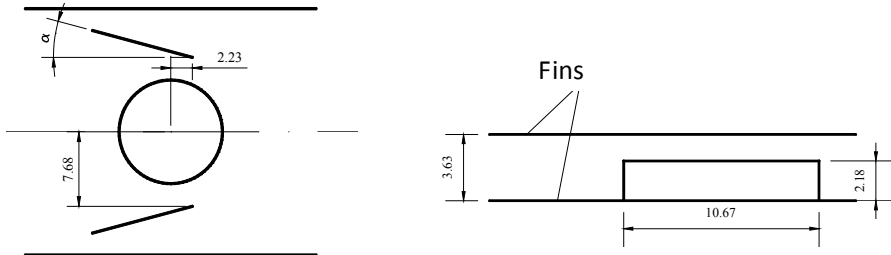


Fig. 55 Dimensions and the placement of LVGs with respect to the tube (unit: mm) [46]

The rectangular winglets are placed on the two sides of the tube using the CFU approach and convergent flow channels are formed between LVGs and the tube wall. The reason that rectangular winglets, instead of delta winglets, are adopted was that more fluid can pass the convergent channel that is similar to a convergent nozzle. The accelerated fluid impinges to the tubes in the next row. The impingement of the fluid reduces the boundary layer thickness and increases the temperature gradient, which ultimately enhance heat transfer. Therefore, the LVGs with CFU placement enhance heat transfer by the combined effects of longitudinal vortices and fluid impingement. The fluid accelerated by the convergent channel not only can enhance heat transfer by impingement, but can also delay the boundary layer separation. Together with the strong swirling secondary flow, the fluid accelerated by the convergent channel can decrease the size of the wake zone to reduce the form drag of the tube. Figure 54 shows the schematic of the core region of a fin-and-tube heat exchanger with rectangular winglets, while Fig. 55 shows the winglet type vortex generator dimensions and the placement with respect to the tube. Due to the low inlet velocity and the small fin pitch, the flow in the channel of the compact heat exchanger is assumed to be laminar and steady. Fin thickness and heat conduction in the fins and vortex generators are taken into account.

### (1) Effect of the angle of attack of the LVGs

Figure 56 shows the different configurations for fin-and-tube heat exchangers without and with rectangular winglets. Four different angles of attack are studied:  $\alpha = 0^\circ$ ,  $10^\circ$ ,  $20^\circ$ , and  $30^\circ$  ( $\alpha = 0^\circ$  corresponds to the baseline case without LVGs).

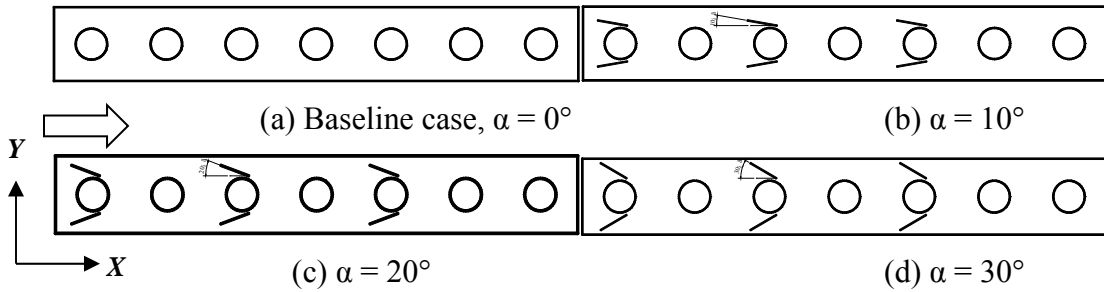
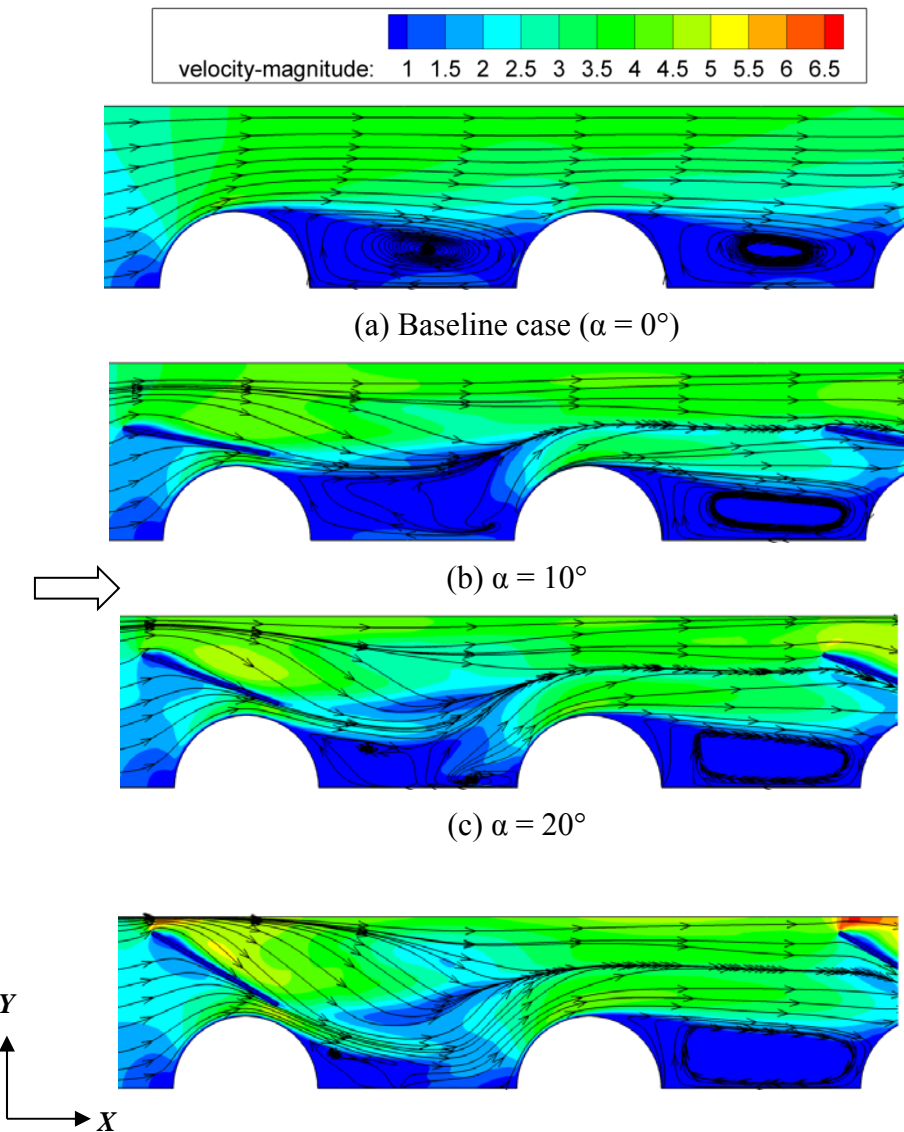


Fig. 56 Different configurations for fin-and-tube heat exchangers with and without rectangular winglets [46]

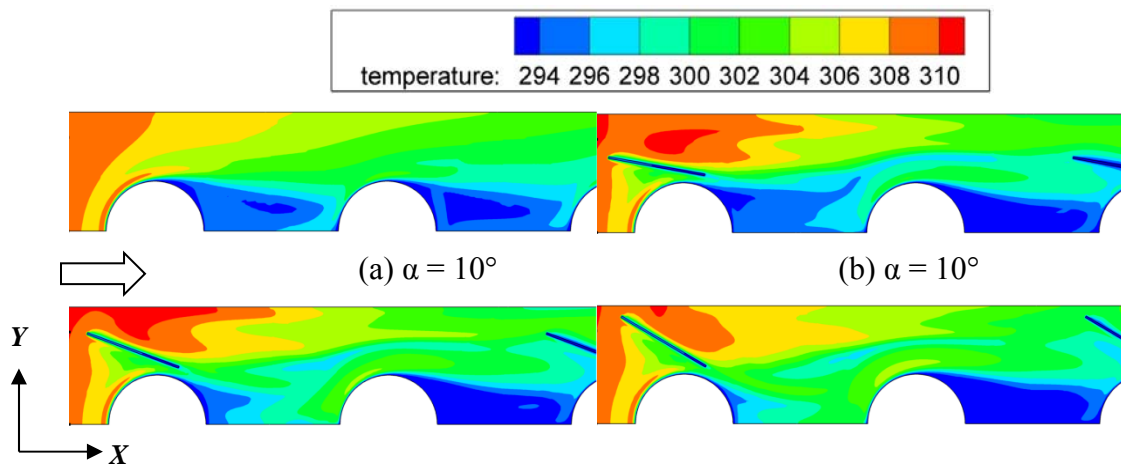


(d)  $\alpha = 30^\circ$

Fig. 57 Velocities and streamlines distribution at different angles of attack ( $Re = 850$ ) [46]

Figure 57 shows the velocity and streamlines distributions at the middle plane perpendicular to the tubes. Due to the periodical feature, the velocity and streamline distributions for the tube rows downstream are similar to that of the first two rows. In order to show the detail of the fluid fields and save space, only the distributions for the first two rows are shown. It can be seen from Fig. 57(a) that the velocity at the downstream of the tube is very low. The pattern of streamlines clearly shows the presence of recirculation patterns in the wake region. The axis of the recirculation flow is perpendicular to the main flow direction so that these recirculation flows are called transverse vortices. They are generated by separation of the fluid from the tube. The transverse vortices independently swirl in the wake zone and are almost isolated from the main flow. On the other hand, it can be seen from Fig. 57(b)-(d) that the streamlines are stretched in the middle of the wake zone. Generation of longitudinal vortices induces high-momentum fluid to the wake zone and decreases the size of the wake zone. As the angle of attack increases, the longitudinal vortices intensify and the streamlines are even more curved in the central region of the wake zone; the size of the wake zone decreases even more. We also found that the LVGs had very little on the heat transfer in the wake zone of the tubes in the next row.

Figure 58 shows the temperature contour at the middle-plane perpendicular to the tube at  $Re = 850$ . For the case without LVGs (Fig. 58(a)), the temperature gradient in the wake zone of the tube is very small. For the cases with LVGs as shown in Fig. 58(b) – (d), the temperature gradient in the wake zone gradually increases with increasing angle of attack. In other words, when LVGs are used, there is better mixing of flow in the wake region so that warm fluid penetrates this zone. Since the wake zone is usually the poorest region for heat transfer in the entire heat exchanger, increasing the mixing in this region results in increase of heat flux and ultimately improves heat transfer. After the fluid flows through the convergent narrow and long channel, it impinges the next tubes in the next row and decreases their boundary thicknesses. The temperature gradient increases, and the heat flux increases, which is very helpful for heat transfer enhancement. As the angle of attack increases from  $0^\circ$  (baseline case) to  $30^\circ$ , the temperature gradient in the region before the tubes in the second row gradually increases because the fluid impingement velocity increases with increasing angle of attack due to increased ratio of the cross-sectional area of the convergent channel. This resulted in thinner boundary layer in front of the tubes in the second row and consequently higher temperature gradient, which reinforced what was found by Sparrow et al. [47].



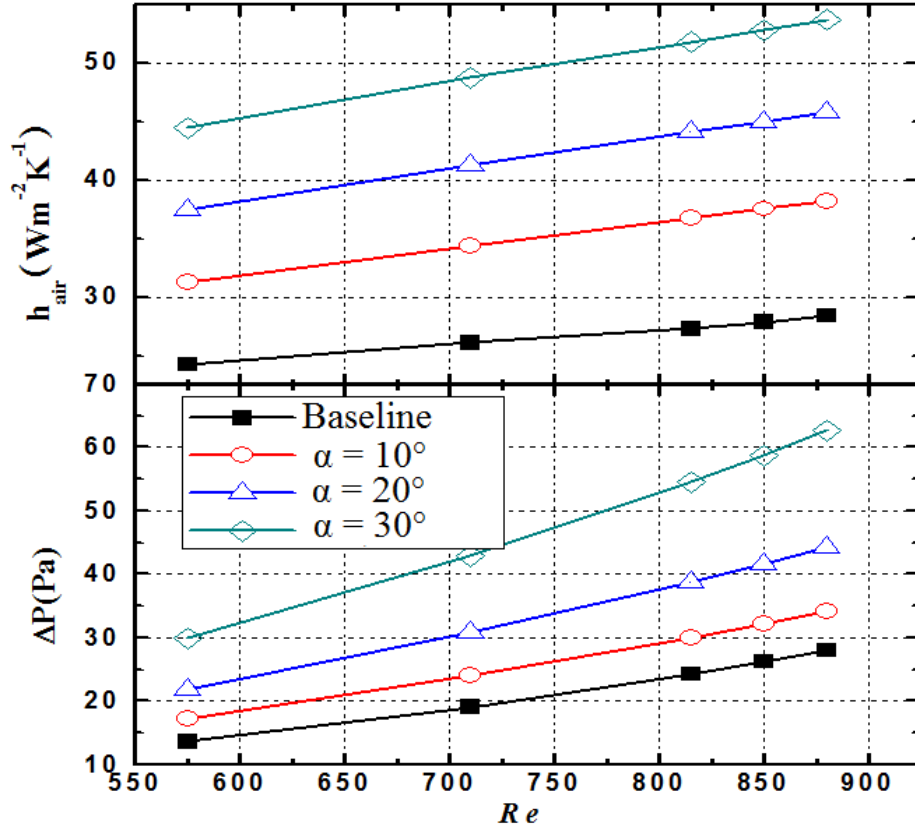
(c)  $\alpha = 20^\circ$ (d)  $\alpha = 30^\circ$ Fig. 58 Temperature distribution at different angles of attack ( $Re = 850$ ) [46]

Fig. 59 Cross-sectional average heat transfer coefficient and pressure drop vs. Reynolds number [46]

Figure 59 shows the average heat transfer coefficient and pressure drop versus Reynolds number at different angles of attack. The air-side heat transfer coefficient is obtained from  $h_{air} = Q / (A \Delta T)$ , where  $Q$  is heat transfer capacity,  $A$  is heat transfer area, and  $\Delta T$  is logarithm mean temperature difference. As can be seen from Fig. 59(a), the heat transfer coefficient increases with Reynolds number since the boundary layer thickness decreases with increasing Reynolds number and the mixing between the hot and cold fluids is promoted by LVGs. Compared to the baseline case and within the range of the Reynolds numbers that was studied ( $Re = 575$ – $880$ ), the heat transfer coefficient on the outside of the tubes is increased by 28.8–34.5%, 54.5–61.5% and 83.3–89.7% for the angles of attack of  $10^\circ$ ,  $20^\circ$ , and  $30^\circ$ , respectively. These results indicate that the rectangular winglets can effectively increase the heat transfer coefficient on the outside of the tube. As can be seen from Fig. 59(b), enhancement of heat transfer is always accompanied by increase of drag. Compared to the baseline case and within the range of the Reynolds numbers that was studied ( $Re = 575$ – $880$ ), the friction factor is increased by 21.9–26.9%, 58.1–61.9% and 119–125% for the angles of attack of  $10^\circ$ ,  $20^\circ$ , and  $30^\circ$ , respectively.

Figure 60 shows the overall performance of the heat exchanger versus Reynolds number at different angles of attack. In the range of Reynolds number studied ( $Re = 575$ – $880$ ),  $j/f$  for the

case of  $\alpha = 10^\circ$  is increased by 1.4–10.3% compared to the baseline case. For the case of  $\alpha = 20^\circ$ , the relative performance of the heat exchanger with LVGs is worse than the baseline case when the Reynolds number is below 800;  $j/f$  for the case with LVGs is higher than the baseline case if the Reynolds number is above 800. The effect of Reynolds number on the overall performance can be explained by its different effects on pressure drops across the tubes and LVGs. As Reynolds number increases, the fluid accelerated by the convergent narrow and long channel achieves higher velocity so that the size of the wake region is reduced and the pressure drop across tubes is decreased. On the other hand, the pressure drop due to LVGs increases with increasing Reynolds number. At higher Reynolds number, decrease of the pressure drop across tubes becomes dominant so that  $j/f$  for the case with LVGs at higher Reynolds number is higher than that of the baseline case. For the case of  $\alpha = 30^\circ$ , the increase of pressure drop due to LVGs for the entire range of Reynolds number is higher than the decrease of pressure drop across the tubes so that the  $j/f$  for the case with LVGs is always lower than that of the baseline case. In the range of Reynolds number that was studied, the overall performance measured by  $j/f$  is 15.5–17.0% lower than that of the baseline case.

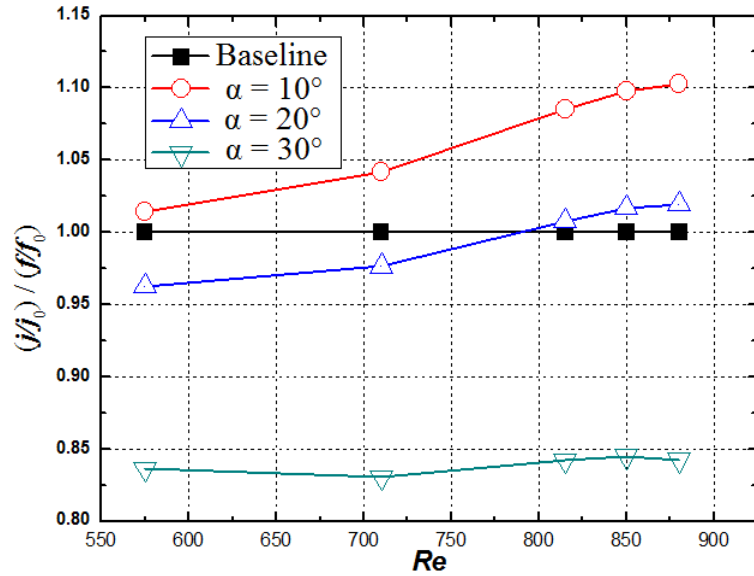


Fig. 60 Relative performances of heat exchangers vs. Reynolds number [46]

It can be concluded from the above discussion that among the four different structures, the heat exchanger with LVGs at angles of attack of  $10^\circ$  and  $20^\circ$  are better than the other two cases. The heat exchanger with LVG at  $\alpha = 10^\circ$  could enhance heat transfer by 30% in comparison to the baseline case while the increase of pressure drop is very small. However, this enhancement does not show any significant advantage over other traditional heat transfer enhancement techniques. On the other hand, the heat exchanger with LVGs at angle of attack of  $20^\circ$  enhances heat transfer by as much as 60% and the heat transfer enhancement at higher Reynolds number ( $Re > 800$ ) is higher than the increase of pressure drop, i.e.,  $(j/j_0)/(f/f_0) > 1$ , which is the most challenging task in heat transfer enhancement. Therefore, the following parametric studies will be carried out for the fin-and-tube heat exchangers with an angle of attack of  $20^\circ$ .

## (2) Effects of the number of LVGs

Figure 61 shows the structures of fin-and-tube heat exchanger with different number of

LVGs, which are rectangular winglet pairs (RWPs). The angle of attack is fixed at  $20^\circ$ , the range of Reynolds number is  $Re = 575\text{--}880$ , and the number of the row of tubes is 7.

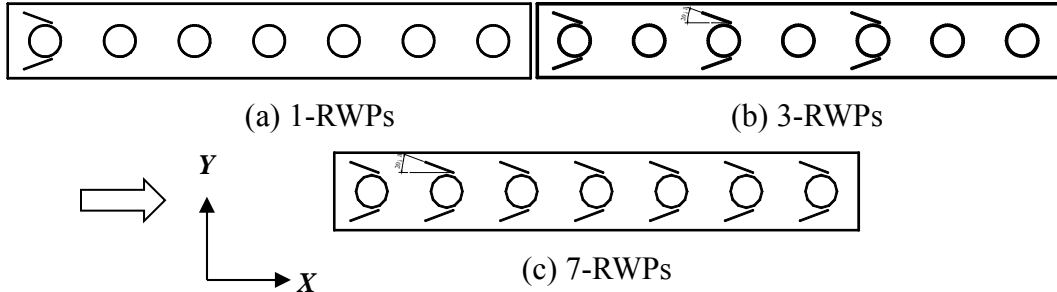


Fig. 61 Fin-and-tube heat exchangers with different numbers of LVGs ( $\alpha = 20^\circ$ ) [46]

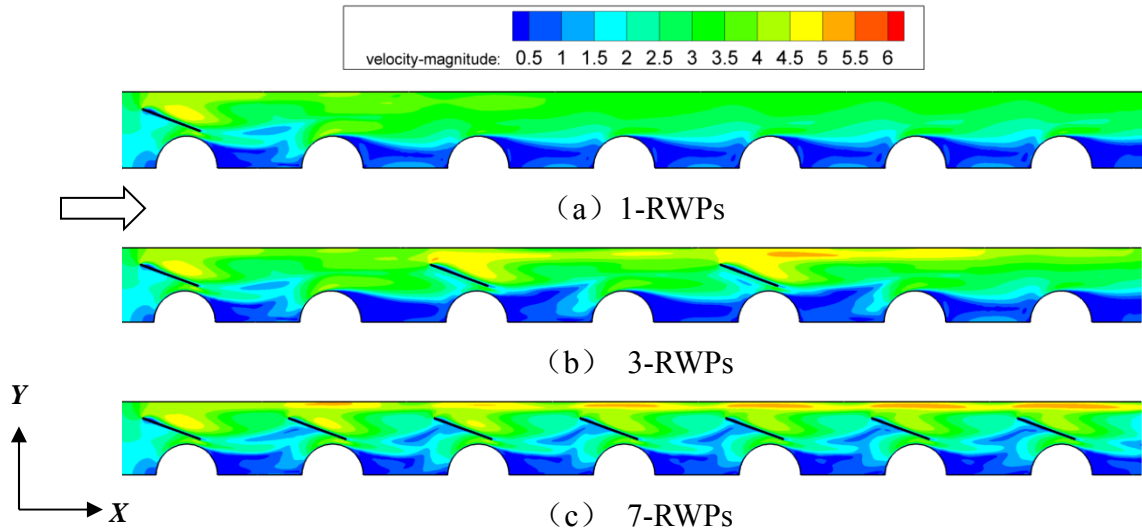


Fig. 62 Distributions of the velocity magnitudes in fin-and tube heat exchangers [46]

Figure 62 shows the distribution of the velocity magnitudes in fin-and tube heat exchangers with different number of LVGs. The high-momentum (or high-velocity) regions can be observed in all 3 different structures. As it was discussed before, when the fluid passes the LVGs, part of it becomes high-velocity swirling secondary flow and part of it is accelerated by the convergent narrow and long flow channel. For the case with one RWP the fluid is accelerated only near the first row of tubes, while for the case with three RWPs the fluid is accelerated near the 1<sup>st</sup>, 2<sup>nd</sup>, and 5<sup>th</sup> rows of the tubes. For the case of seven RWPs, the fluid is accelerated near every row of tubes and the velocity at the downstream of the LVGs gradually increases as the flow gradually develops. It can also be seen from Fig. 62 that due to the strong swirling secondary flow and acceleration by the convergent channel, the size of wake zone behind the first row of the tube for the case of one RWP is significantly decreased. For the case of three RWPs, the size of wake zones behind the 1<sup>st</sup>, 3<sup>rd</sup>, and 5<sup>th</sup> tubes are significantly decreased. When the number of RWPs increases to seven, the sizes of the wake zones behind all seven rows of tubes are decreased. Due to the periodic structure of the flow channel, the wake zones behind all seven rows of tubes are

almost identical.

Figure 63 shows the temperature contours in the fin-and-tube heat exchangers with different numbers of LVGs. It can be seen that the temperature contours for the three structures are almost the same before the first LVG. The temperature gradient behind the first row of the tube for the case of one RWP is higher than that behind the rest of the tubes. For the case of three RWPs, the temperature gradients behind the 3<sup>rd</sup> and 5<sup>th</sup> rows of the tubes is higher than that corresponding to the case of one RWP. Comparison between the cases of three and seven RWPs indicates that the temperature gradient behind every tube for the case of seven RWPs is higher than that for the case of three RWPs. The reason for this difference is that the wake zone behind every (except the 7<sup>th</sup>) tube in the case of seven RWPs is affected by both LVGs located at upstream and downstream. On the contrary, the wake zone behind every tube in the case of three RWPs is affected by only one RWP. Therefore, the wake zones for the case of 7 RWPs are disturbed more and the temperature in the wake zones are also higher.

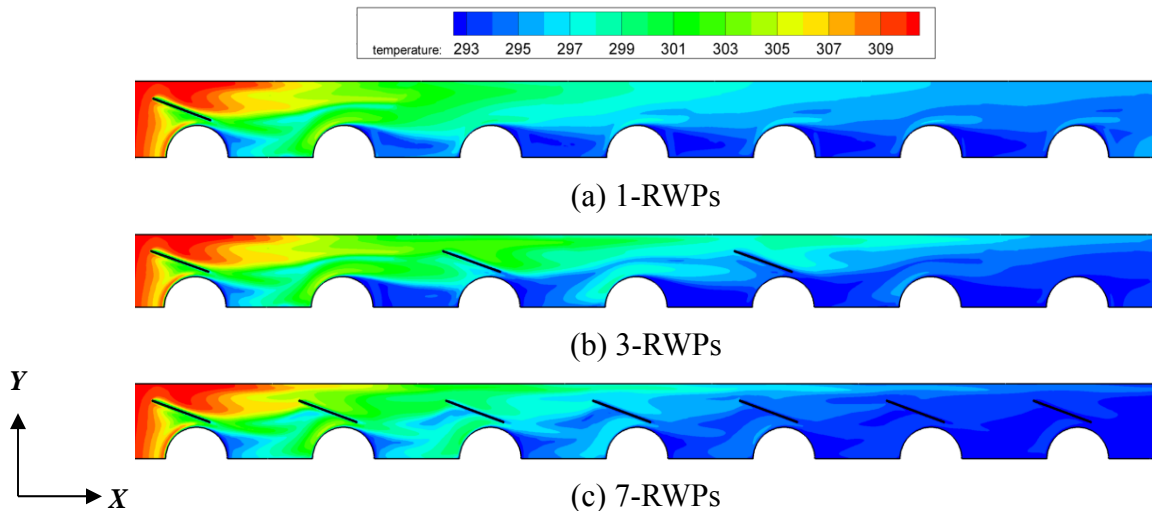


Fig. 63 temperature contours in the fin-and-tube heat exchangers [46]

Figure 64 shows the effect of the number of LVGs on the flow and heat transfer. Comparison between the air side heat transfer coefficients for different number of LVGs is given in Fig. 64(a). Compared to the baseline case, the heat transfer coefficients were respectively increased by 22.7–25.5%, 54.6–61.5 and 87.5–105.1% for the cases of one, three and seven RWPs. While more LVGs result in more significant heat transfer enhancement, the pressure drop also increases with increasing number of LVGs, as indicated by Fig. 64(b). Compared to the baseline case, the pressure drop were respectively increased by 22.0–24.5%, 58.1–62.0 and 123.0–127.6 for the cases of one, three and seven RWPs.

Figure 65 shows the relative heat transfer performance improvement versus Reynolds number for different number of LVGs. It can be seen that for the case of seven RWPs the overall heat transfer performance  $j/f$  in the entire range of Reynolds number is lower than that of the baseline structure. For the cases of one and three RWPs, the overall heat transfer performance  $j/f$  is lower than that of the baseline structure when Reynolds number is under 815, but higher than that of the baseline structure when Reynolds number exceeds 815. Compared to the baseline case, the overall heat transfer performances for the cases of one and three RWPs are increased by 1.7–2.7% and 0.70–2.0, respectively.

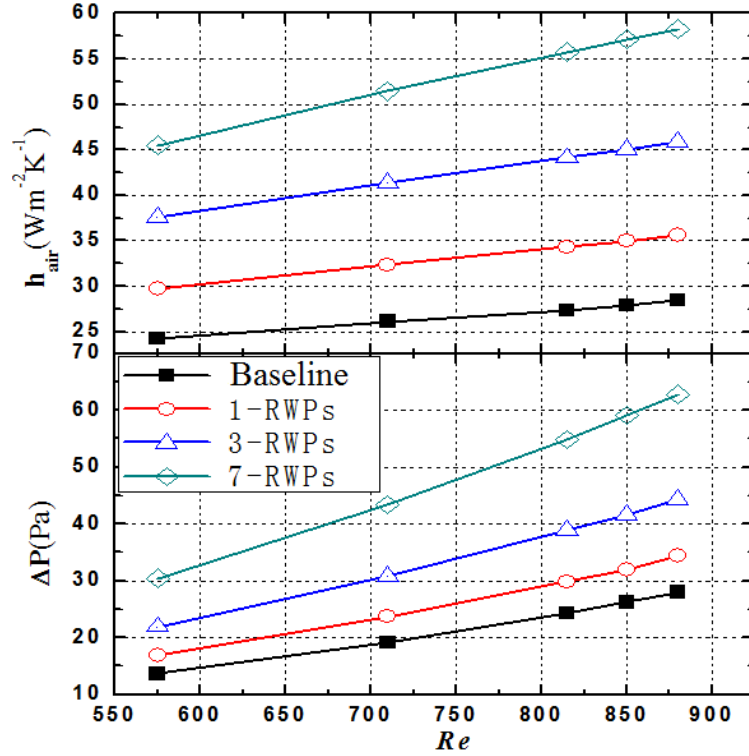


Fig. 64 Heat transfer coefficient and pressure drop vs. Reynolds number [46]

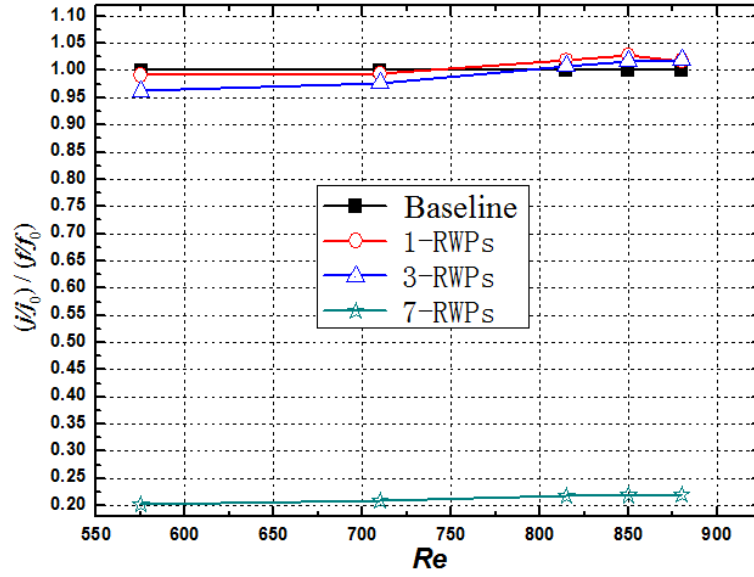


Fig. 65 Overall heat transfer performance versus Reynolds number at different LVG numbers [46]

### (3) Effects of placement of LVGs

Figure 66 shows the schematic of inline and staggered arrangements of LVGs. For the case of inline arrangement of LVGs (see Fig. 66(b)), three pairs (6 total) of rectangular winglets are symmetrically placed on the two sides of the 1<sup>st</sup>, 3<sup>rd</sup>, and 5<sup>th</sup> tubes. For the case of staggered

arrangement of LVGs, the 6 rectangular winglets are alternatively placed on the up and down sides of the tubes 1 to 6. The numbers of rectangular winglets for both arrangements are the same and the angle of attack is  $\alpha = 20^\circ$ . The range of Reynolds number is 575— 880 and the number of rows is 7.

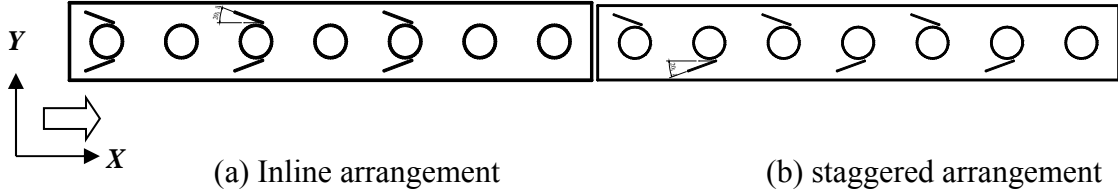


Fig. 66 Inline and staggered arrangements of LVGs [46]

Figure 67 shows the contours of velocities for inline and staggered arrangements of LVGs. For the case of inline arrangement, the velocity is symmetric since the geometric structure of the flow channel is symmetric. Due to the strong swirling flow induced by the LVGs and the impingement of the accelerated flow, the sizes of the wake zones behind the 1<sup>st</sup>, 3<sup>rd</sup>, and 5<sup>th</sup> tubes are somewhat decreased. Since the LVGs are symmetrically placed on the two sides of the tubes, two symmetric high-velocity jets on the two sides of the tube can be formed. However, the velocity components of the two jets in the transverse directions are in the opposite direction so that these two symmetric jets can cancel each other's transverse velocity components. Consequently, the effects of these two jets on the wake zones are weakened and the heat transfer enhancements due to the high-velocity jets are also weakened. On the other hand, the velocity distribution for the case of the staggered LVGs is not symmetric because its geometric structure is not symmetric. Since the six rectangular winglets are staggered on the sides of the 1<sup>st</sup> to 6<sup>th</sup> tubes, every LVG can independently improve the heat transfer in the wake zone behind the tube to its full potential without affected by any other LVGs. While the heat transfer in the wake zones of only three tubes are improved for the case of inline arrangement, the heat transfer for the first 6 tubes are improved at certain degree for the case of staggered arrangement.

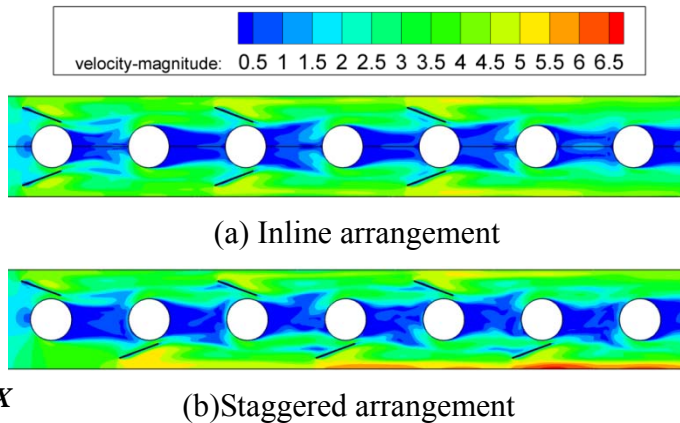


Fig. 67 Comparison of velocity magnitudes for different arrangements of LVGs (unit: m/s; Re = 850) [46]

Figure 68 shows the comparison of the temperature contours for different arrangements of LVGs. For the case of inline arrangement, the temperature is symmetric. The velocities in the wake zones are very low and their mass and energy exchanges with the main flow region are also

very low. Therefore, the fluid temperatures in the wake zones are very close to the tube wall temperatures so that the temperature gradients and heat flux are very low in the wake zones. Due to strong swirling secondary flow and jet impingement effects, the sizes of the wake zones behind the 1<sup>st</sup>, 3<sup>rd</sup>, and 5<sup>th</sup> tubes are significantly decreased. The temperature gradients are increased in these wake zones, which, in turn, helps heat exchange between the tube and the fluid. For the 2<sup>nd</sup>, 4<sup>th</sup> and 6<sup>th</sup> tubes where no LVGs are located, the low heat flux zone extended all the way to the next tube, which degrades the heat transfer performance.

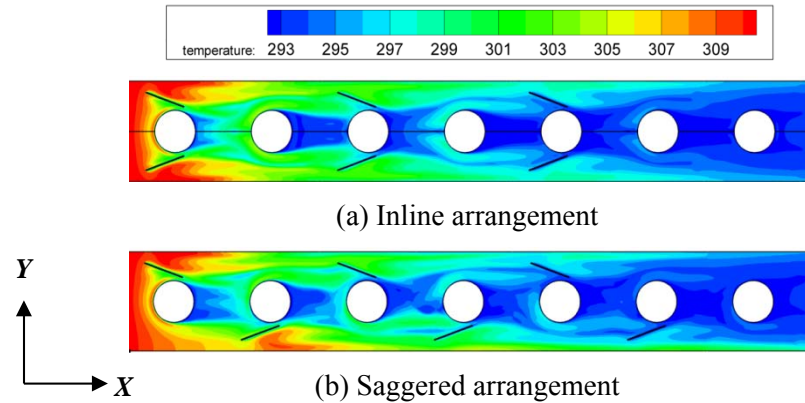


Fig. 68 Comparison of the temperature contours for different arrangements of LVGs [46]

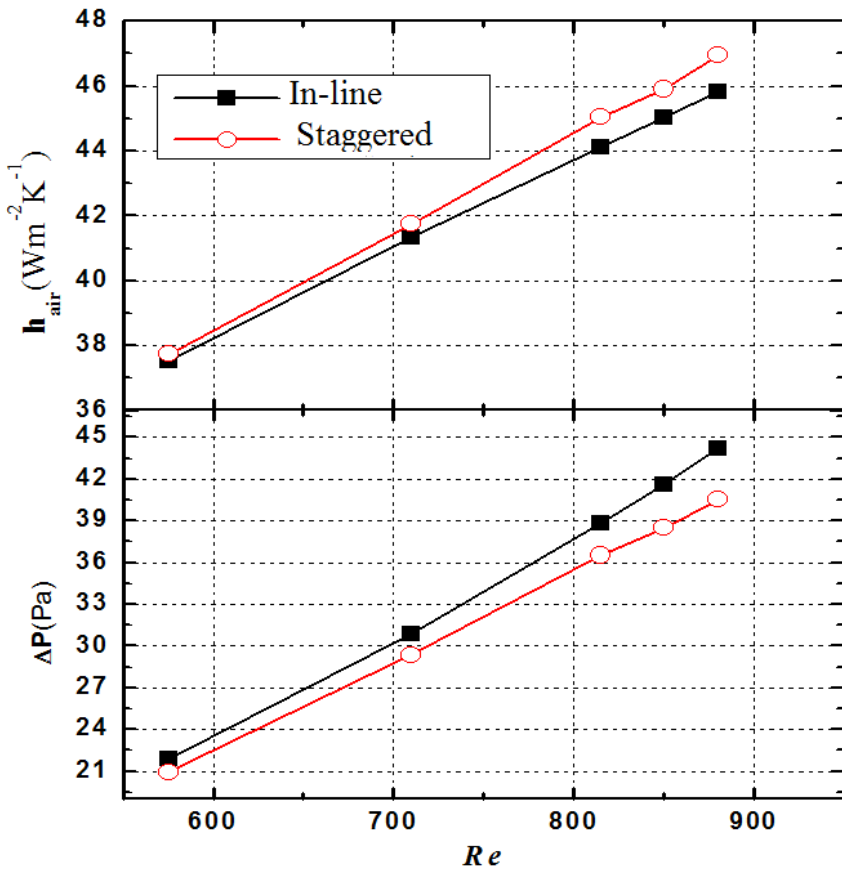


Fig. 69 Comparison of heat transfer and pressure drop for different placement of LVGs

[46]

For the case of staggered arrangement of LVGs, the temperature distribution is not symmetric. Due to the effects of swirling secondary flow and jet impingement, the sizes of the wake zones behind the 1<sup>st</sup> through 6<sup>th</sup> tube are decreased somewhat and the low-heat flux zones becomes smaller; all of these facts attributed to heat transfer enhancement.

Figure 69 shows the comparison of heat transfer coefficients and pressure drop for different arrangements of LVGs. The air-side cross sectional average heat transfer coefficients versus Reynolds number is shown in Fig. 69(a). Compared to the inline arrangement, the air side heat transfer coefficient for staggered arrangement of LVGs is 0.5–2.5% higher. Meanwhile, the pressure drop for staggered arrangement of LVG is 4.5–8.3% lower. Therefore, the staggered arrangement allows further reduction of pressure drop while keeps the level of heat transfer enhancement unchanged, which can be attributed to the asymmetric placement of LVGs. It can be expected that as Reynolds number further increases, the asymmetric structure will further reduce the pressure drop.

#### 4 Conclusions and Outlooks

Compared to the traditional heat transfer enhancement techniques, the LVGs have significant advantages. While the capability of heat transfer is significantly enhanced, the pressure drop only increases by a small degree, or even decreases in some cases. It can achieve the toughest criterion of  $(j/j_0)/(f/f_0) > 1$  that is very difficult to achieve by the traditional measures.

The heat transfer enhancement by LVGs is affected by many factors, such as angle of attack, aspect ratio, locations, arrangement, and flow patterns. Different optimized structures exist depending on the different operating conditions. Since the parameter space for the optimization of LVGs is huge, experimental investigations cannot obtain an optimized design. In addition, the in-depth mechanisms of the heat transfer can only be revealed by analyzing the flow field, and the temperature and pressure distributions. Therefore, it is imperative to use numerical approaches to carry out studies on design optimization of heat exchangers.

Based on the above very detailed review on the state-of-the-art research on heat transfer enhancements by LVGs, we believe that the following three topics will possibly become the “hot spots” for future research:

1. Heat transfer enhancement via LVGs is a passive technique. Due to the continued development of moving mesh techniques, semi-passive heat transfer enhancement techniques deserve more attentions from the researches. The LVGs will be subject to forced vibration due to the fluid pressure, which will further increase the disturbance of the flow field. The disturbance due to vibrations of LVGs can be combined with the swirling secondary flow and jet impingement to further enhance heat transfer.
2. If the LVGs on the fins are manufactured by punching, they will affect the fin efficient to some extent <sup>[48]</sup>. In order to overcome this drawback, Hirokazu <sup>[48]</sup> cut the LVG to two or three sections and studied its performance. The results showed that the fin efficiency is slightly increased and the heat transfer enhancement is increased by 5% and 8% for two and three sections, respectively. Meanwhile, the pressure drop is also slightly decreased. However, the process of manufacturing fins with LVGs becomes complicated when the LVGs are cut into more sections.
3. Further observation of the flow field near the LVGs indicated that when the LVG is cut into

two sections, the first section generates the longitudinal vortex while the second section accelerates the fluid and guides it to the tube in the next row. Based on the above analysis, the LVGs can be improved by the following two aspects. The first aspect is to cut the LVGs to two sections so that they are easy to manufacture and heat transfer can be further enhanced. The second aspect is to combine the delta and rectangular winglets, instead of using only one of them. The first half of the LVG is responsible to generate the longitudinal vortex so that the delta winglet is more appropriate. The second half of the LVG is to guide the flow and accelerate so that rectangular winglet works better. It can be expected that the heat transfer in the fin-and-tube heat exchanger will be further enhanced and the pressure drop can be decreased by using the composite winglets. The heat exchangers with high efficiency and low pressure drop can be obtained.

4. The placement (CFU and CFD) and the locations of the LVGs need to be optimized. Our preliminary study indicated that under the same number of LVGs, the pressure drop can be decreased by 8–10% by changing the placement and locations of the LVGs while keep the same level of heat transfer enhancement. For different heat exchangers, the optimized placements and locations differ. Therefore, it is necessary to thoroughly study the placements and locations of LVGs on various heat exchanger structures so that high-efficiency heat transfer enhancement structures can be obtained.

### Acknowledgements

The present work is supported by the National Natural Science Foundation of China (grant numbers: U0934005 and 51176155), National Basic Research Program of China (973 Program) under grant number 2011CB710702 and the U.S. National Science Foundation (grant number: CBET-1066917). YLH also thanks her former students, Drs. Y. G. Lei, P. Chu and L. T. Tian for their fruitful contributions on this subject during their doctoral studies.

### References

- [1] Bergles AE. ExHFT for fourth generation heat transfer technology[J]. *Experimental Thermal and Fluid Science*, 2002, 26 (2-4): 335-344.
- [2] Fiebig M, Valencia A, Mitra NK. Wing-type vortex generators for fin-and-tube heat exchangers[J]. *Experimental Thermal and Fluid Science*, 1993, 7 (4): 287-295.
- [3] Biswas G, Mitra NK, Fiebig M. Heat transfer enhancement in fin-tube heat exchangers by winglet type vortex generators[J]. *International Journal of Heat and Mass Transfer*, 1994, 37 (2): 283-291.
- [4] Fiebig M. Vortex generators for compact heat exchangers[J]. *Journal of Enhanced Heat Transfer*, 1995, 2 (1-2): 43-61.
- [5] Jacobi AM, Shah RK. Heat transfer surface enhancement through the use of longitudinal vortices - a review of recent progress[J]. *Experimental Thermal and Fluid Science*, 1995, 11 (3): 295-309.
- [6] Gentry MC, Jacobi AM. Heat transfer enhancement by delta-wing vortex generators on a flat plate: Vortex interactions with the boundary layer[J]. *Experimental Thermal and Fluid Science*, 1997, 14 (3): 231-242.
- [7] Fiebig M. Vortices, generators and heat transfer[J]. *Chemical Engineering Research and Design*, 1998, 76 (2): 108-123.

- [8] Torii K, Kwak KM, Nishino K. Heat transfer enhancement accompanying pressure-loss reduction with winglet-type vortex generators for fin-tube heat exchangers[J]. International Journal of Heat and Mass Transfer, 2002, 45 (18): 3795-3801.
- [9] Kwak KM, Torii K, Nishino K. Simultaneous heat transfer enhancement and pressure loss reduction for finned-tube bundles with the first or two transverse rows of built-in winglets[J]. Experimental Thermal and Fluid Science, 2005, 29 (5): 625-632.
- [10] Joardar A, Jacobi AM. A numerical study of flow and heat transfer enhancement using an array of delta-winglet vortex generators in a fin-and-tube heat exchanger[J]. Journal of Heat Transfer-Transactions of the ASME, 2007, 129 (9): 1156-1167.
- [11] Fiebig M, Kallweit P, Mitra N, and Tiggelbeck S, Heat transfer enhancement and drag by longitudinal vortex generators in channel flow[J]. Experimental Thermal and Fluid Science, 1991, 4 (1): 103-114.
- [12] Biswas G, Chattopadhyay H. Heat transfer in a channel with built-in wing-type vortex generators[J]. International Journal of Heat and Mass Transfer, 1992, 35 (4): 803-814.
- [13] Tiggelbeck S, Mitra N, Fiebig M. Flow structure and heat transfer in a channel with multiple longitudinal vortex generators[J]. Experimental Thermal and Fluid Science, 1992, 5 (4): 425-436.
- [14] Tiggelbeck S, Mitra NK, Fiebig M. Experimental investigations of heat transfer enhancement and flow losses in a channel with double rows of longitudinal vortex generators[J]. International Journal of Heat and Mass Transfer, 1993, 36 (9): 2327-2337.
- [15] Tiggelbeck S, Mitra NK, Fiebig M. Comparison of wing-type vortex generators for heat transfer enhancement in channel flows[J]. Journal of Heat Transfer-Transactions of the ASME, 1994, 116 (4): 880-885.
- [16] Fiebig M. Embedded vortices in Internal flow - heat transfer and pressure loss enhancement[J]. International Journal of Heat and Fluid Flow, 1995, 16 (5): 376-388.
- [17] Biswas G, Torii K, Fujii D, and Bishino, K, Numerical and experimental determination of flow structure and heat transfer effects of longitudinal vortices in a channel flow[J]. International Journal of Heat and Mass Transfer, 1996, 39 (16): 3441-3451.
- [18] Dupont F, Gabillet C, Bot P. Experimental study of the flow in a compact heat exchanger channel with embossed-type vortex generators[J]. Journal of Fluids Engineering-Transactions of the ASME, 2003, 125 (4): 701-709.
- [19] Gentry MC, Jacobi AM. Heat transfer enhancement by delta-wing-generated tip vortices in flat-plate and developing channel flows[J]. Journal of Heat Transfer-Transactions of the ASME, 2002, 124 (6): 1158-1168.
- [20] Liou TM, Chen CC, and Tsai, T.W. Heat transfer and fluid flow in a square duct with 12 different shaped vortex generators[J]. Journal of Heat Transfer-Transactions of the ASME, 2000, 122 (2): 327-335.
- [21] Wang QW, Chen QY, Wang L, Zeng M, Huang Y, and Xiao Z, Experimental study of heat transfer enhancement in narrow rectangular channel with longitudinal vortex generators[J]. Nuclear Engineering and Design, 2007, 237 (7): 686-693.

[22] Zhu JX, Fiebig M, Mitra NK. Numerical investigation of turbulent flows and heat transfer in a rib-roughened channel with longitudinal vortex generators[J]. International Journal of Heat and Mass Transfer, 1995, 38 (3): 495-501.

[23] Hiravennavar SR, Tulapurkara EG, Biswas G. A note on the flow and heat transfer enhancement in a channel with built-in winglet pair[J]. International Journal of Heat and Fluid Flow, 2007, 28 (2): 299-305.

[24] Tian LT, He YL, Lei YG, Tao WQ, Numerical study of fluid flow and heat transfer in a flat-plate channel with longitudinal vortex generators by applying field synergy principle analysis[J]. International Communications in Heat and Mass Transfer, 2009, 36 (2): 111-120.

[25] Tian LT, Lei YG, and He YL, Heat transfer enhancement in a channel with longitudinal vortex generators and field synergy principle analysis, Journal of Engineering Thermophysics, 2008, 29 (12): 2128-2130 (in Chinese).

[26] Sommers AD, Jacobi AM. Air-side heat transfer enhancement of a refrigerator evaporator using vortex generation[J]. International Journal of Refrigeration, 2005, 28 (7): 1006-1017.

[27] Leu JS, Wu YH, Jang HY. Heat transfer and fluid flow analysis in plate-fin and tube heat exchangers with a pair of block shape vortex generators[J]. International Journal of Heat and Mass Transfer, 2004, 47 (19-20): 4327-4338.

[28] Allison CB, Dally BB. Effect of a delta-winglet vortex pair on the performance of a tube-fin heat exchanger[J]. International Journal of Heat and Mass Transfer, 2007, 50 (25-26): 5065-5072.

[29] Zhang YH, Wu X, Wang LB, Song KW, Dong YX, Liu S, Comparison of heat transfer performance of tube bank fin with mounted vortex generators to tube bank fin with punched vortex generators[J]. Experimental Thermal and Fluid Science, 2008, 33 (1): 58-66.

[30] Wu JM, Tao WQ. Investigation on laminar convection heat transfer in fin-and-tube heat exchanger in aligned arrangement with longitudinal vortex generator from the viewpoint of field synergy principle[J]. Applied Thermal Engineering, 2007, 27 (14-15): 2609-2617.

[31] Lei YG, He YL, Tian LT, Chu P, Tao WQ, Hydrodynamics and heat transfer characteristics of a novel heat exchanger with delta-winglet vortex generators[J]. Chemical Engineering Science, 2010, 65 (5): 1551-1562.

[32] Sanders PA, Thole KA. Effects of winglets to augment tube wall heat transfer in louvered fin heat exchangers[J]. International Journal of Heat and Mass Transfer, 2006, 49 (21-22): 4058-4069.

[33] Tian LT, He YL, Chu P, Tao WQ, Numerical Study of Flow and Heat Transfer Enhancement by Using Delta Winglets in a Triangular Wavy Fin-and-Tube Heat Exchanger[J]. Journal of Heat Transfer-Transactions of the Asme, 2009, 131 (9): 091901.

[34] Tian LT, He YL, Tao YB, Tao WQ, A comparative study on the air-side performance of wavy fin-and-tube heat exchanger with punched delta winglets in staggered and in-line arrangements[J]. International Journal of Thermal Sciences, 2009, 48 (9): 1765-1776.

[35] Chen Y, Fiebig M, Mitra NK. Conjugate heat transfer of a finned oval tube with a punched longitudinal vortex generator in form of a delta winglet - parametric investigations of the

winglet[J]. International Journal of Heat and Mass Transfer, 1998, 41 (23): 3961-3978.

[36] Chen Y, Fiebig M, Mitra NK. Heat transfer enhancement of a finned oval tube with punched longitudinal vortex generators in-line[J]. International Journal of Heat and Mass Transfer, 1998, 41 (24): 4151-4166.

[37] Chen Y, Fiebig M, Mitra NK. Heat transfer enhancement of finned oval tubes with staggered punched longitudinal vortex generators[J]. International Journal of Heat and Mass Transfer, 2000, 43 (3): 417-435.

[38] Tiwari S, Maurya D, Biswas G, Eswaran V, Heat transfer enhancement in cross-flow heat exchangers using oval tubes and multiple delta winglets[J]. International Journal of Heat and Mass Transfer, 2003, 46 (15): 2841-2856.

[39] O'Brien JE, Sohal MS. Heat transfer enhancement for finned-tube heat exchangers with winglets[J]. Journal of Heat Transfer-Transactions of the ASME, 2005, 127 (2): 171-178.

[40] Herpe J, Bougeard D, Russeil S, Stanciu M, Numerical investigation of local entropy production rate of a finned oval tube with vortex generators[J]. International Journal of Thermal Sciences, 2009, 48 (5): 922-935.

[41] Chu P, He YL, Lei YG, Three-dimensional numerical analysis of fin-and-oval tube heat exchanger with longitudinal vortex generators, Journal of Engineering Thermophysics, 2008, (03): 488-490 (in Chinese).

[42] Chu P, He YL, Tian LT, Lei YG, Optimization and Mechanism of Heat Transfer Enhancement by Longitudinal Vortex Generator, Power Engineering, 2009, (12): 1123-1128 (in Chinese) .

[43] Chu P, He YL, Lei YG, Tian LT, and Li R, Three-dimensional numerical study on fin-and-oval-tube heat exchanger with longitudinal vortex generators[J]. Applied Thermal Engineering, 2009, 29 (5-6): 859-876.

[44] Joardar A, Jacobi AM. Heat transfer enhancement by winglet-type vortex generator arrays in compact plain-fin-and-tube heat exchangers[J]. International Journal of Refrigeration, 2008, 31 (1): 87-97.

[45] Chu P, He YL, Tao WQ. Three-dimensional numerical study of flow and heat transfer enhancement using vortex generators in fin-and-tube heat exchangers[J]. Journal of Heat Transfer-Transactions of the ASME, 2009, 131 (9), 091903.

[46] He YL, Chu P, Tao WQ, Zhang YW, Xie T, 2012, "Analysis of Heat Transfer and Pressure Drops for Fin-and-Tube Heat Exchangers with Rectangular Winglet-Type Vortex Generators," *Applied Thermal Engineering*, DOI: 10.1016/j.applthermaleng.2012.02.040

[47] Sparrow, EM, Chevalier, PW, and Abraham, JP, The Design of Cold Plates for the Thermal Management of Electronic Equipment, Heat Transfer Engineering, 2006, 27(6), 6-16.

[48] Hirokazu F. Research and development on heat exchangers for air conditioners with the alternative winglet[C]. Seventh International Conference on Enhanced, Compact and Ultra-Compact Heat Exchanger: From MicroScale Phenomena to Industrial Applications. Heredia, Costa Rica: Engineering Conferences International, 2009: 201-207.